Am J Physiol Heart Circ Physiol 320: H144–H158, 2021.
First published November 20, 2020; doi:10.1152/ajpheart.00628.2020

american physiological society

AMERICAN JOURNAL OF PHYSIOLOGY
HEART AND CIRCULATORY PHYSIOLOGY

RESEARCH ARTICLE

Environmental Inhalants and Cardiovascular Disease

Acute e-cig inhalation impacts vascular health: a study in smoking naïve subjects

Shampa Chatterjee,[1] Alessandra Caporale,[2] Jian Qin Tao,[1] Wensheng Guo,[3] Alyssa Johncola,[2] Andrew A. Strasser,[4] Frank T. Leone,[5] Michael C. Langham,[2] and Felix W. Wehrli[2]

[1]*Institute for Environmental Medicine and Department of Physiology, University of Pennsylvania Perelman School of Medicine, Philadelphia, Pennsylvania;* [2]*Laboratory for Structural, Physiologic and Functional Imaging, Department of Radiology; University of Pennsylvania Perelman School of Medicine, Philadelphia, Pennsylvania;* [3]*Department of Biostatistics and Epidemiology, University of Pennsylvania Perelman School of Medicine, Philadelphia, Pennsylvania;* [4]*Department of Psychiatry and Center for Interdisciplinary Research on Nicotine Addiction, University of Pennsylvania Perelman School of Medicine, Philadelphia, Pennsylvania; and* [5]*Pulmonary, Allergy, and Critical Care Division, University of Pennsylvania Perelman School of Medicine, Philadelphia, Pennsylvania*

Abstract

This study was designed to investigate the acute effects of nonnicotinized e-cigarette (e-cig) aerosol inhalation in nonsmokers both in terms of blood-based markers of inflammation and oxidative stress and evaluate their association with hemodynamic-metabolic MRI parameters quantifying peripheral vascular reactivity, cerebrovascular reactivity, and aortic stiffness. Thirty-one healthy nonsmokers were subjected to two blood draws and two identical MRI protocols, each one before and after a standardized e-cig vaping session. After vaping, the serum levels of C-reactive protein, soluble intercellular adhesion molecule, and the danger signal machinery high-mobility group box 1 (HMGB1) and its downstream effector and the NLR family pyrin domain containing 3 (NLRP3) inflammasome (as monitored by its adaptor protein ASC) increased significantly relative to the respective baseline (prevaping) values. Moreover, nitric oxide metabolites and reactive oxygen species production decreased and increased, respectively. These observations were paralleled by impaired peripheral vascular reactivity (with reduced flow-mediated dilation and attenuated hyperemic response after a cuff-occlusion test) and metabolic alterations expressed by decreased venous oxygen saturation, postvaping. The current results suggest propagation of inflammation signaling via activation of the danger signaling axis (HMGB1-NLRP3). The findings indicate that a single episode of vaping has adverse impacts on vascular inflammation and function.

NEW & NOTWORTHY Endothelial cell signaling and blood biomarkers were found to correlate with functional vascular changes in a single episode e-cigarettes inhalation in healthy adults. This is indicative of the potential of e-cigarettes (even when inhaled acutely) to lead of vascular dysfunction.

e-cig inhalation; inflammasome; inflammation; oxidative stress; vascular function

INTRODUCTION

Electronic cigarettes (e-cigs) have been promoted as an alternative to conventional cigarettes for the absence of lung carcinogens, tobacco-specific polyaromatic hydrocarbons (tar constituents), and volatile organic compounds (1). However, recent research has shown that e-cig aerosol delivers toxic entities [thermal decomposition products of propylene glycol and glycerol, which include formaldehyde, acetaldehyde; propanal and acrolein (2–5); compounds such as *o*-methylbenzaldehyde, nitrosamines, terpenic compounds, heavy metal, and silicate particles (>1-μm diameter); and ultrafine particles (i.e., structures of <0.1-μm diameter)] to the respiratory system. These penetrate deeply into the respiratory system to reach the alveolar sacs (6, 7). Based on studies in animal models and human subjects, it has become increasingly clear that e-cig aerosol inhalation leads to airway inflammation, oxidative stress, injury, and lung damage (8–11). Inflammation and oxidative stress initiate the process of endothelial dysfunction (EDF), which arises from increased generation of reactive oxygen species (ROS), a decrease in nitric oxide (NO), and formation of cellular adhesion molecules, ultimately leading to vascular disease (12–14).

Correspondence: S. Chatterjee (e-mail: shampac@pennmedicine.upenn.edu).
Submitted 4 August 2020 / Revised 8 November 2020 / Accepted 9 November 2020

In the context of pulmonary disease and EDF, most studies to date have focused on the effects of chronic e-cig exposure (9, 12, 14–16). While such studies have been crucial in detecting an association between e-cig aerosol inhalation and lung disease at a single point in time (17, 18), they are unable to provide information on the earliest signaling events triggered by e-cig inhalation in smoking naïve subjects. Investigating such early events is pivotal in understanding whether initial signaling cues can translate into a functional outcome at a tissue or macroscopic level.

We have thus chosen to investigate acute effects of e-cig usage. Nonnicotinized e-cigs were selected for our studies as nicotine (the stimulant that drives gratification in smokers) delivery in e-cig is highly variable and the effect of nicotine itself would be a major confounder. We reasoned that studying the effects of nonnicotinized e-cigs would highlight the implications of aerosol inhalation alone.

Earlier we reported that a single vaping episode of nonnicotinized e-cig caused pulmonary endothelial activation, oxidative stress, and inflammation in a small cohort of young nonsmoking adults (19). In a separate study, we observed that nonnicotinized e-cig aerosol inhalation compromised vascular function (20). This led us to conclude that even in the absence of nicotine, e-cig aerosol inhalation had detrimental effects on vascular inflammation and function (19, 20). While our study provided valuable information on the signaling events triggered with acute e-cig usage, it was not clear whether the effects of signaling at the microscopic or cellular level translated into observable changes at the macro or vascular level.

We hypothesized that e-cig vaping elicits endothelial inflammation and oxidative stress; these signals on the endothelium can drive functional changes in blood vessels. To test this hypothesis, we evaluated the association between endothelial inflammation and oxidative stress signals and specific MRI parameters of vascular function in smoking naïve healthy subjects who had undergone a combined protocol of noninvasive imaging interleaved with timed blood collections before and after a vaping episode. Indexes of inflammation, endothelial activation, and oxidative stress were assessed by measuring serum C-reactive protein (CRP), soluble intercellular adhesion molecules (sICAM-1), nitric oxide (NO) metabolites (NOx), and reactive oxygen species (ROS). Inflammation-immune signaling was monitored via damage-associated molecular patterns protein and high-mobility group box 1 (HMGB1) and its downstream effector, the NLR family pyrin domain containing 3 (NLRP3) inflammasome (as detected by its adaptor protein ASC, apoptotic speck-like protein containing a caspase recruitment domain). These moieties were examined for association with the MRI metrics (20) within the same cohort.

MATERIALS AND METHODS

E-Cigarettes and Laboratory Reagents

Disposable e-cigs were purchased from ePuffer (New York, NY). This provider was chosen as ePuffer is a popular brand of e-cigs among young adults and because other brands lacked availability of nicotine-free versions. The device consists of a cylindrical lithium battery that supplies 3.7 V to a single-coil atomizer (heating coil) with a resistance of 2.7 Ω. The liquid tank attached to the atomizer is 1.2 mL in volume and is filled with (tobacco flavored) e-liquid composed of 70% pharma-grade propylene glycol (PG) and 30% vegetable glycerine (VG). The atomizer temperature in a similar device has been reported to vary between 145 and 334°C (21).

The ePuffer policy for e-liquids, cartridges, pods, and disposable models that are zero nicotine products is that the liquid used produces vapor and flavor only and no nicotine (0% nicotine means the product is 100% nicotine-free and is manufactured in a nicotine-free environment according to the manufacturer). The ePuffer uses chromatography for every e-liquid flavor and submits a Tobacco Products Directive certification for each product (22).

Purified water from Millipore Nanopure Water systems was used for all assays. Vacutainer tubes were from BD Biosciences (Franklin Lakes, NJ). CellROX Green dye for ROS detection was obtained from Life Technologies (Eugene, OR). Quantikine ELISA kits for CRP and soluble ICAM-1 (sICAM-1) were from R&D Systems (Minneapolis, MN). ELISA kits for HMGB1 and ASC (NLRP3 inflammasome adaptor protein) were from LS Biosciences (Seattle, WA). The colorimetric assay kit for nitric oxide metabolites (nitrate/nitrite) was purchased from Cayman Chemical Co (Ann Arbor, MI).

Study Design

The study was approved by the Institutional Review Board of the University of Pennsylvania, Perelman School of Medicine. All subjects enrolled were adults, and their written informed consent was obtained before participation. Blood sample collection and experiments were carried out in accordance with relevant guidelines and regulations of the University of Pennsylvania, Perelman School of Medicine. Healthy nonsmokers were subjected to an e-cig challenge entailing vaping a nicotine-free e-cig. Nonsmokers underwent two blood draws, before and 1–1.5 h postvaping. The same MRI protocol was repeated before and after the stipulated e-cigarette challenge, lasting ~3–5 min. Overall, the study consisted of two blood draws and two MRI examinations. The first blood draw was followed by MRI; after this the vaping challenge was undertaken. Postvaping (1-1.5 h), MRI and blood draw (in that order) were carried out. The study is registered at ClinicalTrials.gov (March 27, 2018), identifier NCT03479203.

Subject Recruitment for e-Cigarette Vaping Challenge

Thirty-one healthy nonsmokers of both sexes ranging in age from 19 to 33 yr (mean ± SD of 24.3 ± 4.3 yr), and body mass index (BMI) comprised in the range 18.5–30 kg/m^2 were enrolled. Subjects were selected from a pool of individuals who had participated in previous studies in the Department of Radiology and who had also agreed to be contacted for possible participation in future studies. Excluded were pregnant women, individuals with cancer, HIV, mental illness, overt cardio- or neurovascular disease (prior myocardial infarction, stroke, transient ischemic attacks), serious arrhythmias, bronchospastic disease, and upper respiratory tract infection in the past 6 wk. Also excluded were subjects with asthma or similar respiratory diseases. In a visit before the vaping challenge, subjects were asked to complete a

questionnaire to verify the inclusion and exclusion criteria. The subjects were asked to avoid vigorous physical activity within 4 h from the examination and to fast and consume no liquid other than water for at least 8 h before the examination. Subject demographic characteristics including BMI are presented in Table 1.

E-Cig Aerosol Inhalation Protocol

We used a standardized vaping protocol in this study as other methods of monitoring exposure that rely on nicotine content could not be used owing to 0% nicotine in the e-cigs used here. The vaping protocol used conforms to a standardized protocol and was designed based on a data obtained from the average e-cig puffing topography in young adults as reported earlier (19, 20). In general, the average "drag" or puff time on an e-cig device is between 2 and 5 s (23), but studies show that regular e-cig smokers puff or drag for longer duration than smokers (24). We therefore reasoned that a 3-s puff time would better represent the vaping action of first-time e-cig inhalers. Subjects were instructed to drag and inhale in a standardized fashion in the presence of the research coordinator. The paradigm consisted of 16- inhalations or puffs, each 3-s long, during which subjects did not breathe in through the nose. The total time spent on the protocol (including inhalation, release of vapor and a few seconds between puffs) was ~3 min and is equivalent to smoking an entire conventional cigarette. Overall, the protocol represents the average e-cig puffing topography in young adults (19, 25). For control, prevaping values (i.e., the MRI and blood biomarkers for each subject before vaping) were used. The prevaping condition was assumed to not differ from a postsham vaping control, where sham vaping would stand for repeating the puffing paradigm in absence of an e-cigarette, or with the e-cigarette turned off. Because the device we used is turned on automatically through dragging (there is no on/off button), we could not assess the sham vaping. However, in a previous report involving smokers, it was shown that sham vaping or air inhalation was equivalent to the prevaping condition (26). The dose or "amount" of e-liquid inhaled was quantified by weighing to indicate that on average this vaping protocol led to ingestion of about ~0.16–0.2 mg.

Table 1. *Participant demographics*

Variable, units	Nonsmokers
n	31
Sex (M/F)	17/14
Age, yr	24.3 (4.3)[a]
Age range, yr	19-33
BMI, kg/m^2	22.9 (2.4)
BMI range, kg/m^2	18.6–26.6
SBP, mmHg	116.5 (9.6)
DBP, mmHg	68.1 (7.9)
Hct, %	41.6 (3.5)
Race: African American	3
Race: Asian	5
Race: White	23

[a]SD is indicated in parenthesis; BMI, body mass index; SBP, systolic blood pressure; DBP, diastolic blood pressure; hct, hematocrit.

The terms vaping and e-cig aerosol inhalation have been used interchangeably in this report.

Sample (Blood) Collection and Storage (Plasma and Serum)

Two milliliters of blood were drawn before and 1-1.5 h postvaping. The time point postvaping was chosen based on our earlier study that showed that blood-based biomarkers peaked within this time frame and decreased thereafter (19). Plasma and serum were isolated; the former was obtained after centrifugation (2,000–3,000 *g* for 10–15 min) while the latter was obtained after centrifugation of blood postclot formation. Plasma and serum were then stored in 8–10 aliquots at −80°C before analysis. Each aliquot was used for a single assay, and samples were never subjected to any freeze-thaw cycles (19).

Assessment of CRP, sICAM-1 in Serum and HMGB1 and ASC in Plasma

Aliquots of plasma or serum were thawed immediately before analysis. CRP, sICAM-1, HMGB1, and ASC were assayed using quantitative ELISA and quantified using reference curves of standards provided by the manufacturers (R&D Biosystems for CRP, Quantikine Systems for sICAM-1, LS Biosciences for HMGB1 and ASC). Briefly, samples or standards were added to microplates precoated with the antibody to the protein of interest (i.e., CRP or sICAM-1 or HMGB1 or ASC). Antibodies would then bind to the protein in the samples and standards. The unbound substances were washed and removed, and a second antibody specific to the protein to be detected was added. The amount of the second antibody that binds in the microplates is proportional to the CRP or sICAM-1 or HMGB1 amounts present in the initial samples. This antibody is conjugated to horseradish peroxidase; thus a substrate solution that detects horseradish peroxidase activity and that changes color upon binding was used to monitor CRP or sICAM-1 or HMGB1 or ASC. All analyses were completed in triplicate, and data were averaged for all 31 subjects. All data and background microplate values read out by the ELISA plate reader were checked by two separate laboratory personnel. The biomarkers described here are listed in Table 2.

Assessment of Nitric Oxide Metabolites (Nitrate + Nitrite, NOx) in Serum

The measured nitrate/nitrite concentration in serum serves as an index of NO production in the body (27, 28). The concentration of NOx is assessed by means of the Griess reaction (29) using a commercially available nitrate/nitrite colorimetric assay kit. Briefly, 40-μL aliquots of serum were diluted and the nitrate in this aliquot was converted to nitrite. Next, Griess reagent was added to obtain an azo compound that was measured by absorbance colorimetry. Standards provided by the manufacturer were used to quantify NOx in serum.

Cell Culture

Immortalized human pulmonary microvascular endothelial cells (HPMVEC clone ST1.6R) were gifted to one of the authors (S. Chatterjee) by C. J. Kirkpatrick as described previously (30). HPMVECs were plated in Greiner Bio-One Cell

Table 2. *Serum and plasma biomarkers pre- and post-e-cig vaping*

Acronym, units	Biological Meaning	Technique
NOx, μmol/L	Nitrites and nitrates produced from nitric oxide (NO), a potent vasodilatory gas	Colorimetric assay (serum)
CRP, ng/ml	C-reactive protein, marker of systemic and vascular inflammation	ELISA of serum
sICAM-1, ng/ml	Soluble Intercellular adhesion molecules, index of endothelial activation	ELISA of serum
ROS, AFU	Reactive oxygen species, marker of oxidative stress	Fluorescence microscopy of incubated HPMVECs
HMGB1, ng/ml	High mobility group box 1, initiates a pro-inflammatory response	ELISA of plasma
ASC, ng/ml	NOD-, LRR- and pyrin domain-containing protein 3 inflammasome adaptor protein, linked to amplification of inflammation	ELISA of plasma

ELISA, enzyme-linked immunosorbent assay; AFU, arbitrary fluorescence units; HPMVECs, (immortalized) human pulmonary microvascular endothelial cells exposed to 10% serum of the subject.

View Dishes (with glass bottom to enable fluorescence imaging) and cultured using Medium-199 supplemented with 10% FBS, glutamax, antibiotics, and endothelial cell growth supplement (Millipore Upstate). Confluent HPMVECs were treated with Medium-199 supplemented with 10% human serum; 2 h postincubation, the medium was replaced with fresh medium (with fetal bovine serum) and HPMVECs were monitored for ROS production.

Monitoring ROS Production by HPMVECs Using Fluorescence Microscopy

ROS production by HPMVECs was monitored using a ROS-sensitive dye (CellROX Green) and imaged by confocal fluorescence microscopy as reported in some of the authors' prior studies (19, 31). CellROX Green is a cell-permeable, nonfluorescent compound in its reduced form, under control conditions, but reacts with ROS (and free radicals) to get oxidized to a green fluorophore and emits green fluorescence upon excitation at 488 nm. Green fluorescent signal in cells post-Cell ROX treatment is well accepted as indicative of ROS/oxidative stress (19, 32). HPMVECs were labeled with 5 μM CellROX Green for 30 min and imaged by epifluorescence microscopy using a Nikon TMD epifluorescence microscope, equipped a Hamamatsu ORCA-100 digital camera, and Metamorph imaging software (Universal Imaging, West Chester, PA). Images were acquired at $\lambda_{excitation}$ = 488 nm. All images were acquired with the same exposure and acquisition settings as reported previously (19, 33, 34).

Magnetic Resonance Imaging

The magnetic resonance imaging (MRI) data evaluated here in comparison to the biological data derived from blood draws before and after a vaping episode had been acquired previously on the study group of 31 nonsmokers. For detail, see Caporale et al. (20). In brief, the scan protocol included procedures involving three vascular territories: *1*) lower extremity circulation, *2*) brain and *3*) aorta. Physiologic parameters evaluated are listed in Table 3.

First, the purpose of the lower extremity protocol was to evaluate physiological parameters characterizing peripheral vascular reactivity induced by cuff occlusion of arterial and venous circulation at the level of the upper thigh (35). A pneumatic cuff was inflated for 5 min following which femoral artery reactive hyperemia was quantified in terms of the initial acceleration in blood flow [hyperemic index (HI)], peak flow velocity (V_P), time to peak (TTP), and the duration of forward flow (TFF) (35). The concomitant dilation of the femoral artery (flow-mediated dilation or FMD) during hyperemia [luminal flow-mediated dilation (FMD_L)] was evaluated by high-resolution imaging (36). Finally, dynamic changes in venous oxygen saturation (SvO_2) in the femoral vein were recorded concurrently during reperfusion postocclusion.

Second, in the brain, cerebrovascular response to hypercapnia was evaluated in the superior sagittal sinus (SSS; the major draining vein of the cortex). Postexpiratory breath-hold was used as a form of hypercapnic stimulus, as increase in CO_2 partial pressure stimulates vasodilation (37). Blood flow velocity in SSS was acquired continuously during a volitional apnea paradigm comprising three 30 s-breath-holds interspersed with normal breathing (38). Subjects were prompted to follow audiovisual instructions to maximize compliance. A breath-hold index quantifying SSS vasoactive response was evaluated as the slope of blood flow velocity-time curve (i.e., acceleration) following the onset of the stimulus.

Third, aortic arch pulse-wave velocity was quantified as a measure of aortic stiffness. The transit time of the pulse wave from the proximal ascending to proximal descending aorta was determined by quantifying the temporal delay between velocity waves generated from velocity-encoded projections (39). The path length of the pulse wave was determined from an oblique-sagittal image of aorta.

Quantification of Data, Sample Size and Statistical Analysis

The serum (CRP, sICAM) and plasma (HMGB1, ASC) biomarkers were quantitated from the respective ELISA assays using absorbance-concentration curves generated by the standards provided in the kit. NO was quantitated from the total nitrate/nitrite in the serum using a colorimetric standard. For ROS quantification, the fluorescent intensity of images (acquired by MetaMorph) was integrated using ImageJ (National Institutes of Health, Bethesda, MD) analysis software. Integrated intensity was measured within the entire field and background fluorescence subtracted using

Table 3. *Quantitative MRI metrics*

Vascular Territory Targeted/Acronymn units	Physiological Meaning	Technique
Femoral artery		
RI (adim.)	Resistivity index, a measure of vascular resistance	Velocity projections:PI and RI are obtained from the arterial BFV waveform before cuff occlusion (at rest);V_P, TTP, HI, and AUC are obtained from the reactive hyperemia response to cuff occlusion
PI (adim.)	Pulsatility index, a measure of vascular resistance	
HI, cm/s^2	Hyperemic index, or blood flow acceleration during early hyperemia	
V_P, cm/s	Peak blood flow velocity (BFV), or maximum BFV after cuff release	
TTP, s	Time to peak, or time of maximum velocity	
AUC (adim.)	Area under the hyperemic curve	
FMD, %	Luminal flow-mediated dilation, or maximum dilation of the artery during hyperemia	Vessel wall imaging
Femoral vein		
SvO_{2b}, $\%HbO_2$	Baseline SvO_2, or venous blood oxygen saturation before cuff occlusion	Susceptometry-based oximetry
Tw, s	Washout time, or time for oxygen depleted blood to reach the imaged slice	
Upslope, $\%HbO_2/s$	Slope of the resaturation curve	
Overshoot, $\%HbO_2$	Maximum venous resaturation after cuff release referred to the baseline SvO_2	
Superior sagittal sinus		
BHI, cm/s	Breath-hold index, or blood flow acceleration due to hypercapnia	Phase-contrast MRI
Aorta		
PWV, m/s	Pulse wave velocity, pulse wave transmitted upon contraction of the left ventricle	Velocity projections

the threshold tool as reported (33, 40). Data are expressed in arbitrary fluorescence units (AFU).

The concentrations of the six blood-based biomarkers were quantified, and box plots were used to examine their statistical distributions. The change in blood-based biomarkers postvaping was also evaluated as logarithmic fold increase over pre-cig aerosol or baseline. Data are expressed as means ± SD and two-tailed paired *t* tests were used to determine statistical significance. Spearman's and Pearson's correlation between the two metrics (serum biomarkers and qMRI) was evaluated at baseline, postvaping, and between the post- and prevaping differences. Spearman's coefficient (ρ) was used to measure the strength of association between two metrics while Pearson's coefficient (r) was used to evaluate their linear correlation. In the analysis of correlations between the biomarkers and qMRI parameters, log-transformation was performed to account for deviations from normality. Stepwise regression analysis was carried out in SPSS (IBM SPSS Statistics for Windows, version 20, IBM Corp. (Armonk, NY), considering a specific MRI parameter as dependent variable, and testing its functional relation with the ensemble of biomarkers including NOx, CRP, ROS, sICAM-1 (named for simplicity as ICAM-1 in the following formulas), HMGB1, ASC, hematocrit (Hct), and other demographics such as age, BMI, and systolic and diastolic blood pressure (SBP and DBP, respectively). This analysis was performed between the absolute outcomes quantified postvaping, as well as between the relative post- and prevaping changes in MRI parameters and biomarkers respectively, by evaluating the following models:

$$Y_i = f\ (\text{age}, \text{BMI}, \text{SBP}, \text{DBP}, \text{Hct}, \text{NOx}, \text{CRP}, \text{ROS}, \text{ICAM-1}, \text{HMGB1}, \text{ASC}) \quad (1)$$

$$\Delta Y = f\ (\text{age}, \text{BMI}, \text{SBP}, \text{DBP}, \text{Hct}, \Delta\text{NOx}, \Delta\text{CRP}, \Delta\text{ROS}, \Delta\text{ICAM-1}, \Delta\text{HMGB1}, \Delta\text{ASC}) \quad (2)$$

where Y_i represents the specific MRI parameter i, and Δ represents the post- versus prevaping difference. Hematocrit, age, BMI, SBP, and DBP were quantified once, prevaping or at baseline. The confidence intervals were set at 95%, and pairwise exclusion was applied in case of missing variables. Stepwise regression is shown in Table 4.

RESULTS

Blood-Based Markers of Inflammation and ROS Production

E-cig aerosol inhalation led to a change in all the blood-based biomarkers monitored postvaping. Serum CRP, sICAM-1, and plasma HMGB1 and ASC (Figs. 1 and 2) showed an increase in all subjects, postvaping. CRP, HMGB1, and ASC increased in all subjects, sICAM-1 in 90% of subjects, and NO was decreased (Fig. 3, *A* and *C*), in 80% of the subjects. These observations indicate that post-e-cig inhalation, the circulatory system experienced an "inflammation load" (i.e., an accumulation of inflammation moieties that would be in direct contact with the vascular network). We therefore evaluated the potential of the serum in subjects (pre- and postvaping) to initiate oxidative stress in the pulmonary endothelium. HPMVECs treated with medium

Table 4. *Stepwise regression analysis coefficients*

	Regression Model	Coefficients (Nonstandardized) ± SD	95% CI	Significance (*P*)
FMD	FMD = a × Hct + b × CRP + k	a = −0.84 ± 0.21	(−1.27, −0.42)	<0.0001
		b = −1.54 ± 0.45	(−2.45, −0.62)	0.002
		k = 50.17 ± 9.30	(31.07, 69.28)	<0.0001
PWV	PWV = a × age + b × ASC + k	A = 0.12 ± 0.039	(0.038, 0.20)	0.005
		b = −1.18 ± 0.53	(−2.26, −0.09)	0.035
		k = 5.22 ± 1.16	(2.85, 7.60)	<0.0001
BHI	BHI = a × Hct + b × age + c × BMI + d × DBP	a = −0.018 ± 0.004	(−0.027, −0.010)	<0.0001
		b = −0.014 ± 0.004	(−0.021, −0.007)	0.001
		c = 0.017 ± 0.006	(0.004, 0.030)	0.011
		d = −0.004 ± 0.002	(−0.008, 0)	0.045
ΔBHI	ΔBHI = a × BMI + k	A = 0.008 ± 0.004	(0, 0.016)	0.039
		k = −0.206 ± 0.087	(−0.39, −0.027)	0.025

ASC, adaptor protein of the NLRP3 inflammasome; BHI, breat-hold index; BMI, body mass index; CRP, C-reactive protein; DBP, diastolic blood pressure; FMD, flow-mediated dilation; hct, hematocrit; PWV, pulse wave velocity.

supplemented with serum from subjects pre- and postvaping yielded ROS production (Fig. 3, *B* and *D*). Each subject showed a unique fluorescence signal profile pre- and postvaping; however, in all cases an increase in ROS postvaping was detected. ROS increase is visually displayed via fluorescence micrographs as seen in Fig. 3*E*. The integrated fluorescence intensity across the microscopic fields in Fig. 3*E*, was used to quantitate the amount of ROS generated by HPMVECs in Fig. 3*B*.

Two observations stand out across all 31 nonsmokers recruited for this study: *1*) there was a large intersubject variation in the baseline values for each of the measured biomarkers, with CRP ranging from 4.7–1,826 ng/mL, sICAM-1 108–351 ng/mL, HMGB1 7.3–13.3 ng/mL, ASC (representing the adaptor protein of NLRP3 inflammasome) 0.36-5 ng/mL, NOx 15.5–103.5 μmol/L, and ROS 296.5–3061.9 arbitrary fluorescence units (AFU); *2*) there was a large variability in the response to the e-cig challenge, in terms of the "change in biomarkers": ΔCRP varying from 2.8–1,593.0 ng/mL, ΔsICAM-1 4.8–148.3 ng/mL, ΔHMGB1 0.1–26.7 ng/mL, ΔASC 0.4–5.9 ng/mL, ΔNOx −62.2 to −9.3 μmol/L, and ΔROS 115.3–5102.0 AFU.

As shown in Figs. 1–3, all biomarkers evaluated post-e-cig challenge were significantly different with respect to the baseline levels (log transformations were used in case of non-normality). Furthermore, the *n*-fold change in each marker across all 31 subjects showed a change relative to baseline that was adjusted to unity (means ± SD, CRP ∼1.2 ± 0.1, sICAM-1∼ 1.03 ± 0.03, HMGB1∼ 1.12 ± 0.14, ASC ∼1.3 ± 0.5, ROS ∼1.1 ± 0.06, and NOx ∼0.95 ± 0.7).

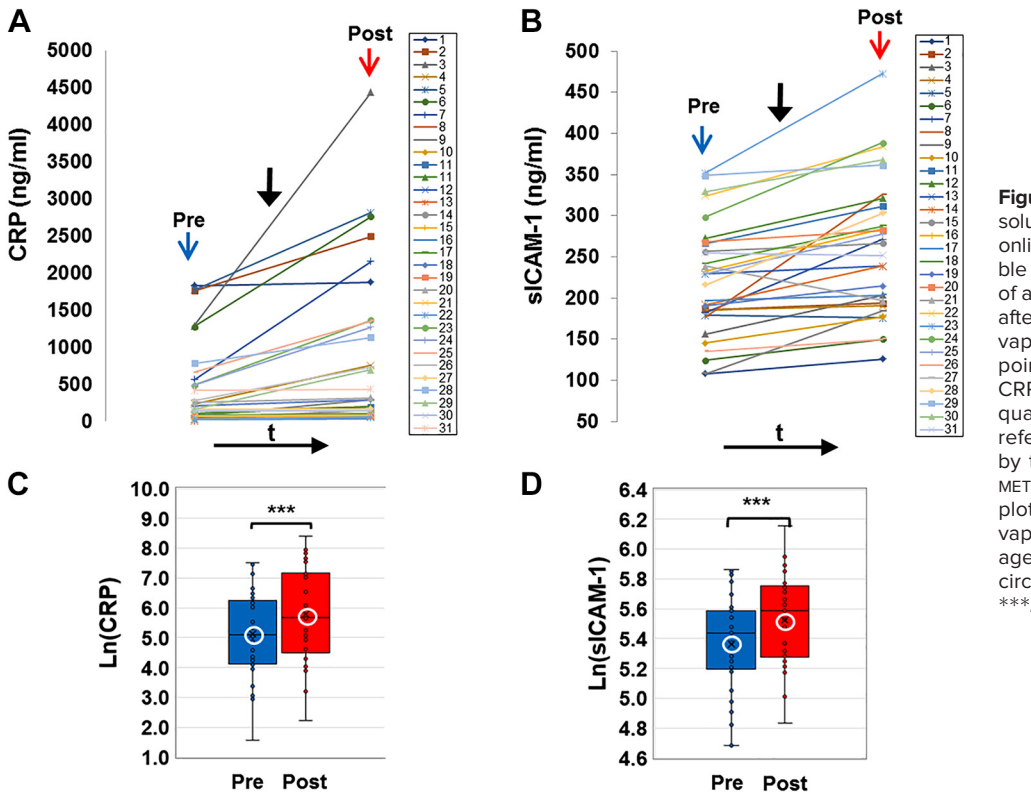

Figure 1. C-reactive protein (CRP) and soluble ICAM-1 (sICAM-1) in serum (colored online). *A* and *B*: profiles of CRP and soluble ICAM-1 (sICAM-1) extracted from serum of all subjects before (pre, blue arrow) and after (post, red arrow) e-cigarette (e-cig) vaping. Solid black arrow denotes the point in time of e-cig aerosol inhalation. CRP and ICAM-1 were assayed using quantitative ELISA and quantified using reference curves of standards provided by the manufacturer (see MATERIALS AND METHODS). *C* and *D*: box and whiskers plots of CRP and sICAM-1 pre- and postvaping, plotted in log scale. Group average and median are indicated by white circle and horizontal bar, respectively; ***$P < 0.0005$.

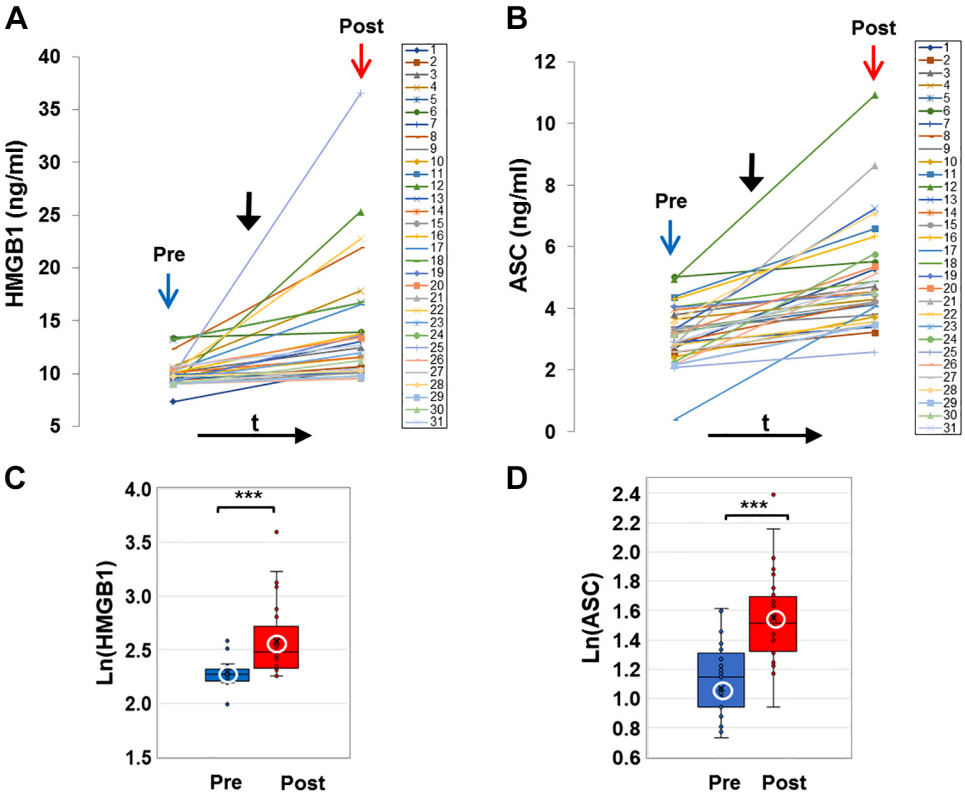

Figure 2. Damage-associated molecular patterns (DAMP) protein, high-mobility group box 1 (HMGB1), and ASC, the adaptor protein of the NLR family pyrin domain containing 3 (NLRP3) inflammasome in plasma (colored online). *A* and *B*: profiles of HMGB1 and ASC extracted from the plasma of all subjects before (pre, blue arrow) and after (post, red arrow) e-cigarette (e-cig) vaping. Solid black arrow denotes the point in time of e-cig aerosol inhalation. HMGB1 and ASC were assayed using quantitative ELISA and quantified using reference curves of standards provided by the manufacturer (see MATERIALS AND METHODS). *C* and *D*: box and whiskers plots of HMGB1 and ASC pre- and postvaping, plotted in log scale. Group average and median are indicated by white circle and horizontal bar, respectively; ***$P < 0.0005$.

Effect of e-Cig Vaping on Quantitative MRI Markers of Endothelial Dysfunction

Our prior analysis of MRI metrics had indicated that e-cig aerosol inhalation affected the hyperemic response to cuff-occlusion in the femoral artery and vein in the same group of healthy nonsmokers examined in the current study (for details, see Ref. 20). Briefly, postvaping femoral artery FMD_L was reduced (−34%, $P < 0.001$) and so was the maximum hyperemic velocity and the blood flow acceleration (−20% and −26%, respectively, $P < 0.001$), relative to prevaping values. Furthermore, indexes of vascular resistance postvaping such as postvaping resistivity index (RI) and pulsatility index (PI) were found to have increased postvaping in 71% and in 75% of the subjects, respectively, suggesting increased resistance to blood flow in the peripheral vascular bed. These observations from our prior study paralleled the currently observed decrease in postvaping NOx levels (Fig. 3*A*). The significant decrease in NO between pre- and postvaping (Fig. 3*C*) implies reduced NO bioavailability and is in line with compromised vasodilation, expressed by FMD decrease and with increased resistance of blood flow to the peripheral vascular bed postvaping.

As previously reported, postvaping oxygen saturation measured before the cuff-occlusion test in the femoral vein (SvO_{2b}, where "b" here denotes baseline i.e., SvO_2 estimated before cuff occlusion) was 20% lower, and overshoot, corresponding to maximum resaturation postcuff occlusion, was 50% higher (both $P < 0.001$), whereas the upslope did not vary between pre- and postvaping. Cerebrovascular reactivity to hypercapnia in the superior sagittal sinus, expressed by BHI, trended lower postvaping, albeit without reaching significance ($P = 0.08$). Finally, there was a marginally significant alteration in arterial stiffness as indicated by a 3% pulse wave velocity increase postvaping ($P = 0.05$).

Associations within the Biomarkers of Inflammation and Oxidative Stress

From the examination of the blood draws taken pre-e-cig aerosol inhalation, HMGB1 and its downstream effector ASC were positively associated (Spearman's $\rho = 0.45$, $P = 0.01$, Fig. 4*A*). These two biomarkers cooperate to form the HMGB1-NLRP3 axis, responsible of the initiation and amplification of inflammation. In addition, ASC showed a weak positive relation with ROS ($\rho = 0.37$, $P = 0.04$, Fig. 4*B*) indicating that redox status is linked to NLRP3 inflammasome activation. Postvaping the only significant association observed within biomarkers was between CRP and NOx ($\rho = -0.43$, $P = 0.015$, Fig. 4*C*).

The magnitudes of alteration of the various inflammation markers pre- and post-e-cig aerosol inhalation, evaluated as $\Delta Y = Y(post) - Y(pre)$, with Y the specific biomarker, were not associated with one another.

Associations between Biological and MRI Markers

Before e-cig vaping challenge (baseline).

ROS (as detected via fluorescence microscopy in HPMVECs exposed to the serum of nonsmokers at baseline) was significantly correlated with the pulsatility index (PI), a measure of vascular resistance distal to the femoral artery ($\rho = 0.49$, $P = 0.005$; Fig. 5*A*). NOx levels showed a negative trend with PI at baseline and were correlated with pulse or heart rate (HR)

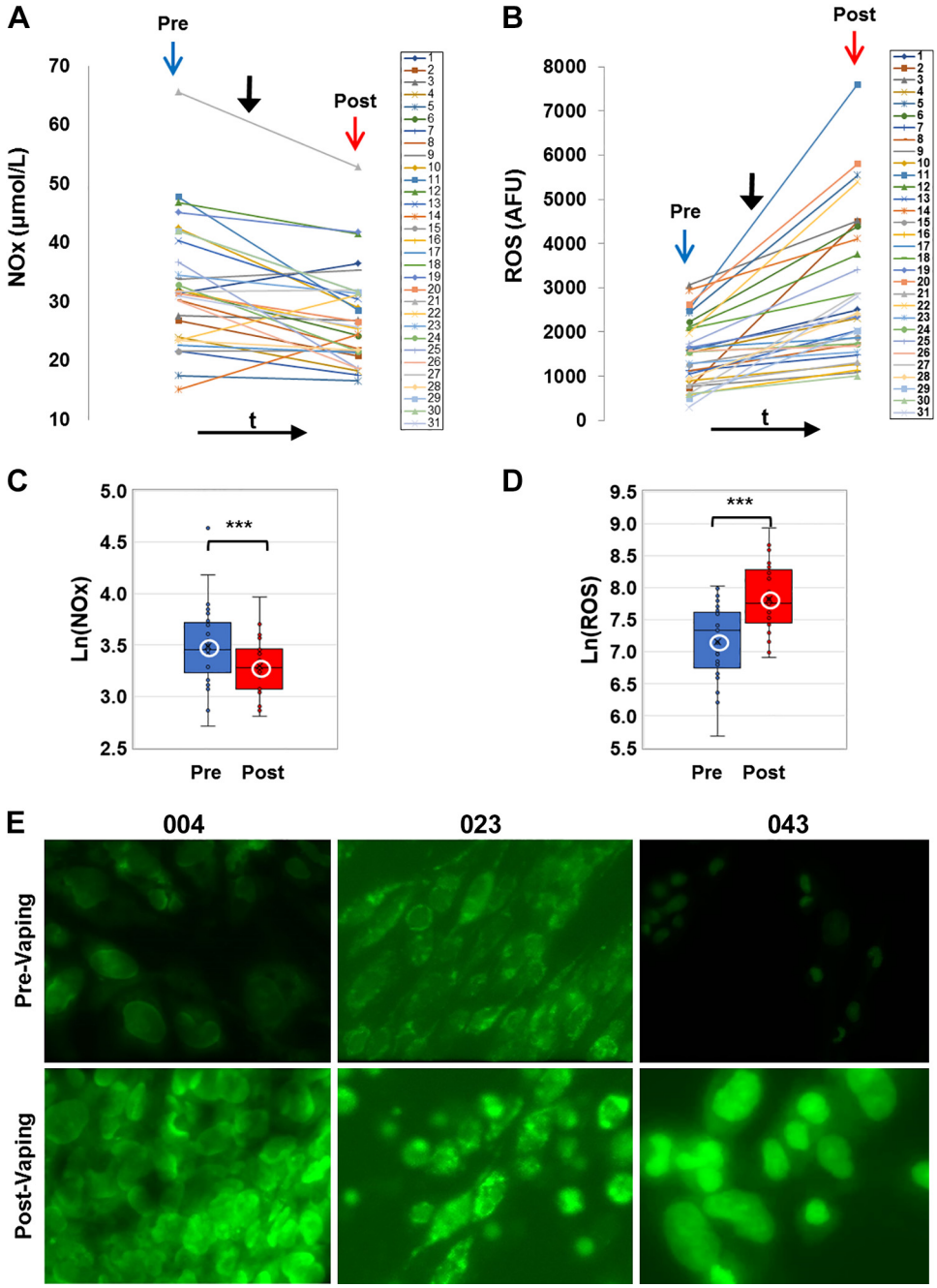

Figure 3. Nitrate-nitrite (NOx) in serum and reactive oxygen species (ROS) production. *A* and *B*: profiles of NOx and ROS for all subjects before (pre, blue arrow) and after (post, red arrow) e-cig vaping. Solid black arrow denotes point in time of e-cigarette (e-cig) aerosol inhalation. Serum samples were assayed for NOx colorimetrically using a nitrite-nitrate Griess reaction assay and NOx was quantified by standard curves. ROS production was quantified via fluorescence intensity measurements (see MATERIALS AND METHODS). *B*, *inset*: box and whiskers plots of ROS, plotted in log scale (***$P < 0.0005$). *C* and *D*: box and whiskers plots of NOx pre- and postvaping, plotted in log scale. Group average and median are indicated by white circle and horizontal bar, respectively; ***$P < 0.0005$. *E*: human pulmonary microvascular endothelial cells exposed to media with 10% serum extracted pre- and post-e-cig vaping. Results from 3 sample subjects (*004*, *023*, and *043*) are shown. The cells were labeled with CellROX Green fluorescent dye, sensitive to ROS production. Cells were imaged on the stage of a microscope at λex 488 nm, λem 500-560, max ~530 nm. All images were acquired at the same settings on Nikon Axiophot microscope using Metamorph Imaging Software. AFU, arbitrary fluorescence units.

(Fig. 6*A*). sICAM-1 was inversely related with RI (ρ = −0.43, P = 0.02, Fig. 5*B*) and positively with SvO_2 upslope (ρ = 0.39, P = 0.03, Fig. 6*A*).

Associations between post- and prevaping changes in biomarkers and MRI metrics.

Inspection of the "post-pre" differences (Δ) of the MRI metrics in relation to the changes in blood-based biomarkers (Supplemental Figs. S1 and S2, available at https://doi.org/10.6084/m9.figshare.12753449 and https://doi.org/10.6084/m9.figshare.12753461) showed that the variation in HMGB1 (ΔHMGB1) was inversely related to Δovershoot and ΔPI (ρ = −0.37, P = 0.04 in both cases) and proportional to the variation in pulse rate (HR), measured from the arterial pulsatile blood velocity waveform (ρ = 0.37, P = 0.04). Stepwise regression analysis indicated that the variation in BHI due to the e-cig challenge was significantly associated with BMI. Nonstandardized coefficients, with their respective significance and confidence intervals, are reported in Table 4. The analysis also indicated functional dependence between ΔPI and ΔROS. The association between ΔROS and Δovershoot was not significant (see Supplemental Table S1, available at https://figshare.com/articles/dataset/Supplemental_Table_1/13096619).

After e-cig vaping challenge.

Serum CRP evaluated in the second blood draw (1-1.5 h postvaping) correlated negatively with superficial femoral artery

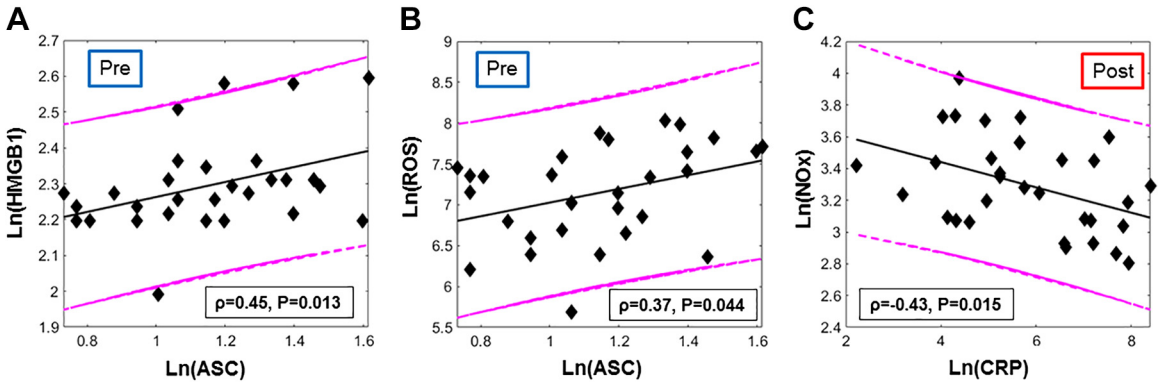

Figure 4. Fig. 4. Associations between blood-based biomarkers (colored online): *A*: high-mobility group box 1 (HMGB1) and ASC levels in plasma extracted from the blood-draw executed before e-cigarette (e-cig) vaping challenge ("pre"). *B*: reactive oxygen species (ROS) production and ASC concentration quantified before e-cig vaping. *C*: nitrate-nitrite (NOx) and C-reactive protein (CRP) levels in serum quantified from the blood-draw executed after the e-cig vaping challenge and the second MRI protocol. Spearman's correlation coefficients and the respective *P* values are reported in the box; 95% prediction and regression lines are indicated. Log transforms were used since the data were not normally distributed

FMD, elicited by cuff occlusion and reperfusion, in the postvaping MRI session ($\rho = -0.41$, $P = 0.02$; Fig. 5*D*). Stepwise regression analysis indicated a significant functional dependence of FMD on both Hct and CRP, as shown in Table 4. In addition, postvaping, the hyperemic peak velocity (V_P) and the area under the hyperemic curve (AUC) were found to scale with CRP levels ($\rho = 0.42$, $P = .02$; $r = 0.45$, $P = 0.01$), and $\rho = 0.40$, $P = 0.03$, respectively) (Fig. 5*F*). HMGB1 levels postvaping correlated with MRI metrics extracted from reactive hyperemia, time to peak (TTP) and hyperemic index (HI) ($\rho = -0.49$ for TTP and $\rho = 0.49$ for HI, $P = 0.007$, Fig. 5*E*). HMGB1 correlated with overshoot ($\rho = -0.46$, $P = 0.01$), i.e., venous O_2 saturation exceeding baseline, following cuff release. This relation was well described by a linear model ($r = -0.49$, $P = 0.007$, with r Pearson's correlation). ROS produced postvaping correlated with PI quantified after vaping ($r = 0.47$, $P = 0.008$; Fig. 5*C*). Stepwise regression analysis showed that pulse wave velocity (PWV) measured after vaping was significantly related to both age and the postvaping value of NLRP3 (Table 4). The functional dependence between PWV and age is in agreement with a previous study (41). Finally, the breath-hold index (BHI) measured postvaping was related to age, BMI, and Hct.

DISCUSSION

This is a first report where changes at the cellular level were evaluated for associations with functional vascular changes in the context of e-cig inhalation. Studies to date on physiological implications of e-cig vaping have either focused on cellular changes or macro changes and less on the links between the two (42, 43). Although causative associations between endothelial cellular and systemic vascular effects are a well-accepted concept in other models of vascular disease (44, 45), a direct association has not been documented for e-cig inhalation. Furthermore, most of cellular to organ associations are complicated due to confounding factors arising from chronic e cig usage; our study departs from such models by using an acute inhalation episode in nonsmoking/vaping subjects to evaluate the micro- to macro-link without any effects from other variables that can affect vascular health.

In general, e-cig inhalation has been reported to damage endothelial cells (12, 14) and to affect vascular function (43, 46). Randomized studies of acute and chronic e-cig users and nonusers have shown e-cig vaping can lead to increased arterial stiffness in humans and rodents (43, 47, 48). Indeed, our early studies on a single vaping episode have shown endothelial signaling (inflammation and oxidative stress) (19) and altered vascular function as captured by MRI metrics, sensitive to endothelial function and representative of peripheral and cerebrovascular reactivity (20). In testing our hypothesis that e-cig vaping elicits endothelial inflammation and oxidative stress and that these signals are able to provoke changes in blood vessels that can potentially affect vascular function, we observed an association between several moieties (biomarkers) at the cellular level and functional changes at the whole-organ (vascular bed) level.

The significant increase in several major players of inflammation [CRP, HMGB1, and NLRP3 inflammasome (as assessed from increase in adaptor protein ASC)], oxidative stress (ROS), and endothelial activation (sICAM-1) after vaping indicates an inflammatory response and oxidant production. The acute-phase inflammatory, highly conserved, plasma protein CRP (that exhibits elevated expression in the blood during inflammatory conditions ranging from cardiovascular diseases to infection) was found to increase by 20–25% (Fig. 1), which is comparable to inflammatory disorders (49).

The damage-associated molecular pattern protein HMGB1 and its downstream effector NLRP3 are known to elicit a strong proinflammatory response (50). The observation that the change in HMBG1 with vaping is close to values observed in patients with mild forms of infection (51, 52) is indicative of the severity of the inflammatory response with e-cig consumption. HMGB1 has been reported as one of the agonists of NLRP3 inflammasome activation. The NLRP3 inflammasome is assembled following stimulation; assembly involves combination of NLRP3, its adaptor protein ASC, and procaspase 1. In general, inflammasome proteins have great potential to be used as biomarkers of injury and disease; indeed, blood ASC

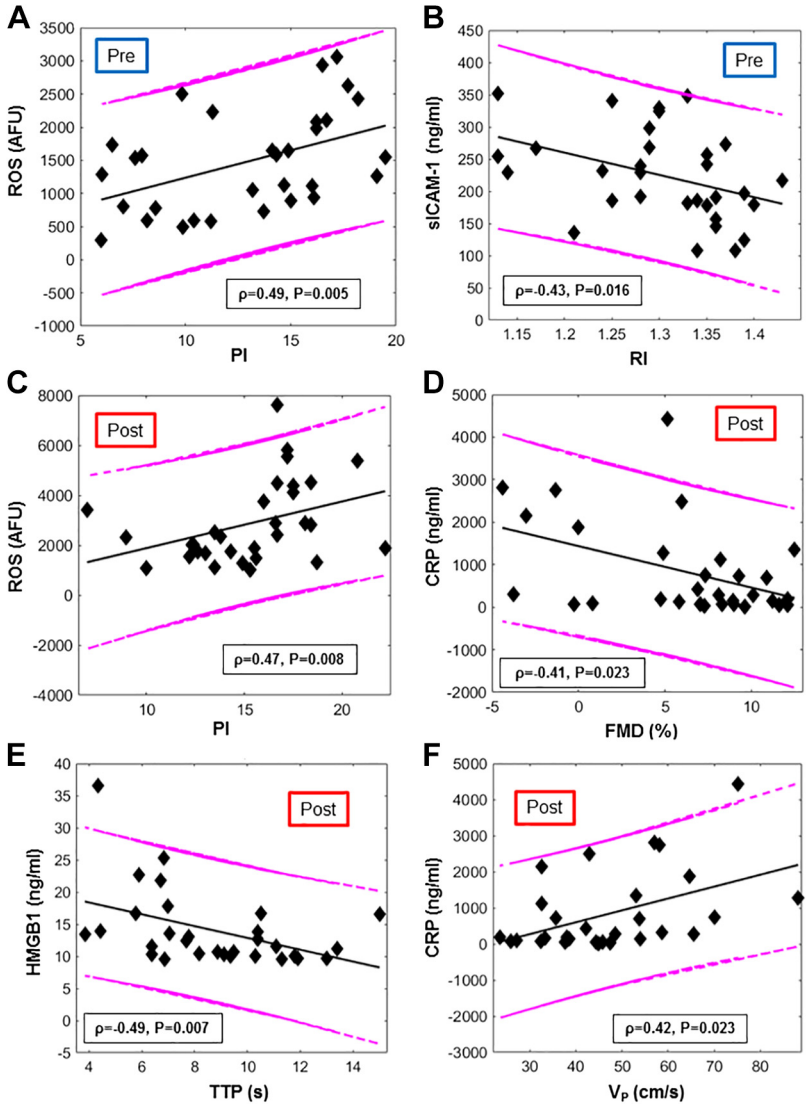

Figure 5. Correlation between blood-based markers and MRI metrics (colored online). Scatterplots of biomarkers plotted vs MRI metrics, evaluated before (pre) and after (post) e-cig vaping. *A* and *C*: reactive oxygen species (ROS) vs Pulsatility Index (PI) respectively, before and after e-cig vaping. *B*: intercellular adhesion molecules (sICAM) vs resistivity index (RI). *D*: C-reactive protein (CRP) vs luminal flow-mediated dilation (FMD). *E*: high mobility group box 1 (HMGB1) vs. time to peak velocity during hyperemia (TTP). *F*: CRP vs. peak hyperemic velocity (V_P). The Spearman's correlation coefficients and respective *P* value are provided, along with 95% prediction intervals and regression lines.

has been reported as a reliable biomarker of inflammation (53, 54). The activation of this pathway following a single episode of e-cig aerosol inhalation indicates that such acute exposure is sufficient to trigger the inflammation machinery that is known to perpetuate cell injury. At baseline, i.e., pre-vaping, these two biomarkers, HMGB1 and adaptor protein ASC, showed a positive association (Fig. 4*A*). As the HMGB1-NLRP3 inflammasome pathway are part of a classical "immune sensing" pathway, such a correlation may be expected. However, contrary to expectation, postvaping there was no association between HMGB1 and ASC; this could arise from different activation profiles of the two moieties.

Increased ROS generation by HPMVECs (a human lung endothelial line) was observed here as reported in a pilot study (19). Other authors found that a single use of nicotinized e-cig caused over 50% increase in 8-iso-prostaglandin, a marker of oxidative damage, indicating peroxidation of membrane phospholipids (42). The increase in ROS production as observed by us was concomitant with the decrease in NOx (Fig. 3, *A* and *B*). Reduction in NOx which represents NO levels, is a key feature and trigger for endothelial dysfunction. NO production has been reported to decline via reduced endothelial nitric oxide synthase (eNOS) expression, or post-translational regulation of eNOS activity, or by reaction with ROS. However, the lack of correlation between ROS and NOx seems to indicate that the reduced NOx post-e-cig inhalation is possibly due to altered eNOS. The soluble form of ICAM (sICAM-1) that is shed from the surface of activated pulmonary endothelial cells along the vascular wall and alveolar epithelium represents the "adherent" capacity of the endothelial layer of the vascular wall. sICAM-1 in serum provides insights into early events of leukocyte recruitment. In clinical studies, sICAM-1 has been reported to show a 40% increase in patients with slow coronary blood flow (55). While lower than in these inflammation conditions, the 15–20% increase in ICAM-1 that we observed, in response to a single episode of e-cig aerosol inhalation, is indicative of an inflammatory state.

These biomarkers were poorly associated to each other, presumably because the signaling processes driving the expression of each of them are not linked in the specific "stress-stimulus" provided here (single exposure to nonnicotinized e-cig aerosol). This is unlike several chronic smoking-related

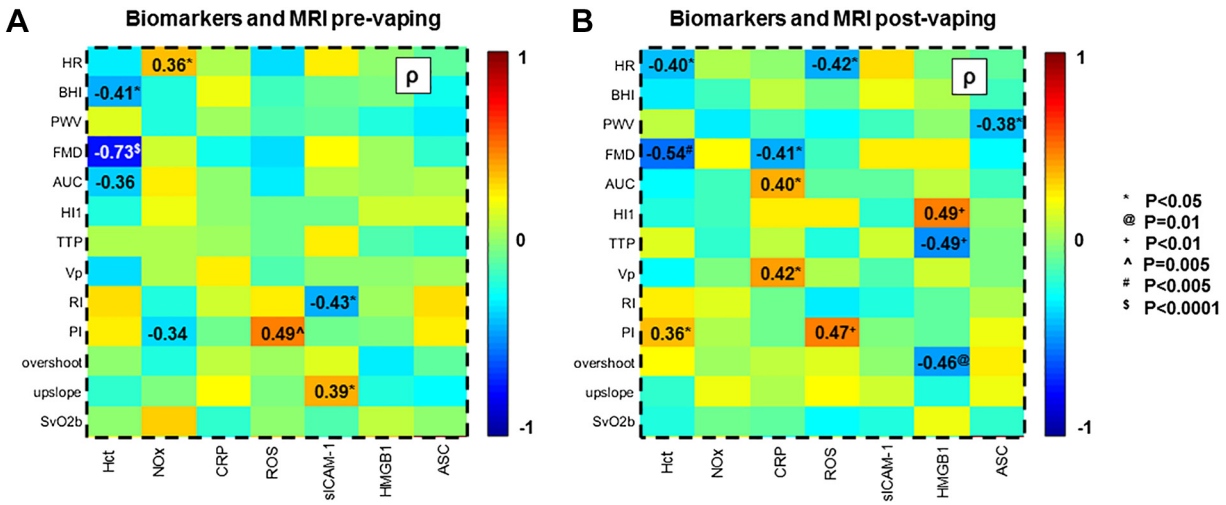

Figure 6. Heatmaps of associations between biomarkers and MRI metrics. *A* and *B*: colormaps showing Spearman's correlation coefficients ρ of the various associations between biomarkers and MRI metrics acquired respectively before and after the e-cig vaping challenge. Comparison pairs are indicated in bold for *P* values <0.05 (see key for actual *P* values). Acronyms are listed in Tables 2-, and 3. Notice that the association between flow-mediated dilation (FMD) and hematocrit (Hct) refers to prevaping.

inflammation conditions, where blood-based biomarkers correlate with one another (56, 57). Furthermore, poor association could reflect the fact that the kinetics of production and degradation of each of these moieties are different and thus measurements in systemic circulation 1 to 1.5 h postvaping may not "capture" the exact concentrations of these inflammation moieties as they are generated in response to e-cig aerosol inhalation.

The considerable variation in baseline levels of inflammation moieties (especially CRP and ASC) and oxidative stress markers (ROS, NOx) could be due to differences in age, sex, weight, lipid levels, blood pressure, fitness, and antioxidant status (58). Furthermore, baseline CRP levels can vary greatly in individuals due to other factors, including polymorphisms in the CRP gene (59). Up to 50% of baseline variance in CRP is associated with the number of dinucleotide repeats found in an intronic region of the gene (60). We observed that not only CRP at baseline but also the response in terms of CRP increase after e-cig vaping challenge were comparable in a couple of twins, as part of the study group of nonsmokers. For these twins, the CRP levels at baseline (482.9 and 478.9 ng/mL) differed less than 1% (0.8%), and their response to the vaping challenge differed less than 7% (CRP levels measured postvaping were 1356.9 and 1267.5 ng/mL). The large intersubject variations in ROS production postvaping possibly reflect the individual differences in the response to an oxidative challenge. Indeed, responses to oxidants have been found to depend on the antioxidant status of human subjects (61).

We investigated the associations of the biomarkers and MRI metrics in several ways: prevaping (baseline), post-e-cig vaping and finally considering the association between the differences (i.e., ΔY and ΔZ, with Y the specific biomarker and Z the MRI parameter). As expected, baseline NOx (which represents nitric oxide derived metabolites present in the systemic circulation) correlated inversely with pulsatility index (PI), an indicator of vascular resistance. ROS production was positively correlated with PI, both pre- and post-e-cig vaping: in fact, ROS drives endothelial activation and under chronic conditions represents increased vascular resistance via remodeling. Our results thus suggested that PI quantified in the superficial femoral artery is sensitive to oxidative stress. A positive relation between lipid peroxides, a type of ROS, and PI of uterine arteries (measured via Doppler ultrasound) was found elsewhere in a cohort of women with preeclampsia (62), a common pregnancy complication characterized by high blood pressure. Another index of vascular resistance, RI, was found to be associated with sICAM-1, indicative of transiently compromised vascular health. Furthermore, we noticed that the endothelium-dependent vasodilatation, expressed by femoral artery FMD, was dependent on the hematocrit (Hct) level at baseline. FMD in the superficial femoral artery is essentially NO-mediated (63). It is known that hemoglobin can interact in vitro with the vasodilatory factor NO via oxidation, addition, and *S*-nitrosylation (64, 65).

Postvaping, serum CRP was found to be correlated negatively with FMD. A negative relation between brachial artery FMD and serum inflammatory markers CRP and TNF-α had been previously found in patients with impaired cardiac function (66). Elsewhere, vascular diameter (but not FMD per se) has been found to be significantly reduced with increased CRP in the systemic circulation (67). The reason why this would occur postvaping needs to be determined; however, the CRP-FMD correlation in our study indicates that the inflammatory load in the systemic circulation post-e-cig inhalation is sufficient to compromise flow-mediated changes in the vasculature. Furthermore, CRP was inversely correlated with NOx in serum postvaping ($\rho = -0.43$, $P = 0.02$), possibly suggesting diminished anti-inflammatory protection with increased NO scavenging (68). Finally, we found that HGMB1 and the overshoot of the dynamic O_2 saturation curve following cuff release were inversely correlated postvaping. The overshoot represents the venous oxygen saturation exceeding the metabolic needs of the tissue, during reperfusion after cuff-induced transient occlusion of femoral artery and vein (see Ref. 20). We conjecture that for those subjects experiencing a stronger proinflammatory response (represented by HMGB1), the

metabolic needs of the hypoxic tissue were higher, or more likely, the efficiency in reperfusion was lower.

While significant correlations between several MRI metrics and blood-based markers were found when compared in pre- and postvaping settings, the change (post-pre) in the biomarkers was generally not associated with the change in MRI metrics. This is not surprising as taking differences always magnifies the noise (from biological and instrumental variability) and change (post-pre) cannot be accurately reflected in maneuvers that are not temporally aligned. However, significant functional relationships between MRI metrics and biomarkers (FMD and CRP; overshoot and ROS) indicate that CRP can play a role in affecting FMD. Similarly, the production of ROS by endothelial cells could be a possible compensatory response by the vessel to drop in oxygenation (overshoot).

In terms of demographics, BMI and age had an (expected) significant functional relationship with vascular reactivity (BHI), as both age and metabolic disorders accompanying increasing BMI are known to affect vascular function (69).

In Caporale et al. (20), it was shown that in the absence of an e-cig challenge, two identical MRI procedures (with cuff-occlusion) performed 10–20 min apart yielded similar MRI metrics, demonstrating excellent repeatability. Postvaping, MRI biomarkers correlated with several blood-based biomarkers (Fig. 5, *C–F*, and Fig. 6*B*) indicating the possibility that e-cig inhalation driven inflammation and oxidative stress can lead to altered vascular properties in vivo.

Although the correlation between inflammation/oxidative stress markers and MRI indexes revealed that cellular changes can lead to alterations at the macroscopic level, there are some inherent limitations of this due to which a direct correlation of biomarkers and cellular signals with vascular function cannot be made. A direct functional link necessitates an identical maneuver for all measures and the evaluation of the effect of inhibition of cellular inflammation/oxidative stress on vascular function. In addition, the blood based inflammatory markers measured are systemic and MRI indexes represent a "local" vascular bed (femoral artery, femoral vein, superior sagittal sinus, aortic arch). For practical reasons associated with the vaping and imaging protocol, "post-pre" measurements of biomarkers and MRI metrics are temporally coincident (i.e., prevaping blood draw is done at baseline while postvaping blood draw occurs after vaping and 2 MRI cuff occlusion procedures), and this may account for lack of significant associations between the differences in biomarkers and MRI-metrics. Furthermore, the endothelial cell model used to monitor oxidant production with vaping was an approximation of the in vivo vascular bed.

This study does not inform on the impact of nicotine and flavored e-cig-driven endothelial changes on vascular function. The effects of nicotine in e-cig aerosol have been somewhat conflicting; while in vitro studies show that e-cig aerosol with nicotine causes significantly high proinflammatory effects and endothelial permeability as compared with nicotine free aerosol (70), in vivo studies on mice report that e-cigs without nicotine had more detrimental effects on endothelial function, markers of oxidative stress, inflammation, and lipid peroxidation than e-cig aerosol containing nicotine (14). However, in chronic smokers, e-cig inhalation induced micro- and macrovascular dysfunction, and oxidative stress was attributed to nicotine alone (12). Flavorings do not affect the rate of nicotine delivery (71) but produce varying effects on endothelial dysfunction and inflammation, depending on the specific flavoring (16, 72). Comparable or additional toxicity (in terms of endothelial dysfunction, lung inflammation, lipid-based immune mediators, and alter lung immunophenotype) of the flavoring chemicals over PG/VG e-cig aerosol has been reported (73). These reports indicate that nicotine and flavorings would lead to an enhanced endothelial dysfunction, oxidative stress, and inflammation as compared with nonnicotinized e-cigs; we theorize that altered vascular function would parallel these changes. Presumably, the association between changes at the micro- level and the outcome at the macroscopic level would be stronger than that observed with nonnicotinized e-cig aerosol inhalation.

CONCLUSIONS

Inflammation and oxidative stress response involving the HMGB1-NLRP3 (ASC) pathway and ROS production post-e-cig aerosol inhalation correlated with several parameters of vascular function indicating that transient changes in inflammation and oxidative stress signals following a single episode of nonnicotinized e-cig vaping affect vascular function at a holistic level. The effects seen are transient occurring on a time scale of hours, and therefore, no inferences can be made on long-terms consequences of repeated vaping nor are the exact toxins known that elicit the observed immune response. However, the observed correlations between the cellular signaling (i.e., biological markers) and vascular function in vivo are suggestive that vaping can potentially lead to adverse long-term alterations in vascular function in the vaping population.

ACKNOWLEDGMENTS

We thank Kelly Sexton and Holly Stefanow for help with recruitment and enrollment of the study subjects.

GRANTS

This research was supported by National Heart, Lung, and Heart Grant R01-HL139358.

DISCLOSURES

No conflicts of interest, financial or otherwise, are declared by the authors.

AUTHOR CONTRIBUTIONS

S.C., A.A.S., F.T.L., and F.W.W. conceived and designed research; S.C., J.T., and A.J. performed experiments; S.C., A.C., and M.C.L. analyzed data; S.C., A.C., W.G., and F.W.W. interpreted results of experiments; S.C. and A.C. prepared figures; S.C. and A.C. drafted manuscript; S.C., A.C., W.G., A.A.S., F.T.L., and F.W.W. edited the original and revised manuscript; S.C., A.C., J.Q.T., W.G., A.J., A.A.S., F.T.L., M.C.L., and F.W.W. approved final version of the manuscript.

REFERENCES

1. **Hecht SS.** Lung carcinogenesis by tobacco smoke. *Int J Cancer* 131: 2724–2732, 2012. doi:10.1002/ijc.27816.

2. **Cibella F**, **Campagna D**, **Caponnetto P**, **Amaradio MD**, **Caruso M**, **Russo C**, **Cockcroft DW**, **Polosa R.** Lung function and respiratory symptoms in a randomized smoking cessation trial of electronic cigarettes. *Clin Sci (Lond)* 130: 1929–1937, 2016. doi:10.1042/CS20160268.
3. **Dinakar C**, **O'Connor GT.** The health effects of electronic cigarettes. *N Engl J Med* 375: 1372–1381, 2016. doi:10.1056/NEJMra1502466.
4. **Goniewicz ML**, **Knysak J**, **Gawron M**, **Kosmider L**, **Sobczak A**, **Kurek J**, **Prokopowicz A**, **Jablonska-Czapla M**, **Rosik-Dulewska C**, **Havel C**, **Jacob P**, **Benowitz N 3rd.** Levels of selected carcinogens and toxicants in vapour from electronic cigarettes**.** *Tob Control* 23: 133–139, 2014. doi:10.1136/tobaccocontrol-2012-050859.
5. **Margham J**, **McAdam K**, **Forster M**, **Liu C**, **Wright C**, **Mariner D**, **Proctor , C.** Chemical composition of aerosol from an e-cigarette: a quantitative comparison with cigarette smoke. *Chem Res Toxicol* 29: 1662–1678, 2016. doi:10.1021/acs.chemrestox.6b00188.
6. **Korfei M.** The underestimated danger of E-cigarettes-also in the absence of nicotine. *Respir Res* 19: 159, 2018. doi:10.1186/s12931-018-0870-4.
7. **Pisinger C**, **Dossing M.** A systematic review of health effects of electronic cigarettes. *Prevent Med* 69: 248–260, 2014. doi:10.1016/j.ypmed.2014.10.009.
8. **Madison MC**, **Landers CT**, **Gu BH**, **Chang CY**, **Tung HY**, **You R**, **Hong MJ**, **Baghaei N**, **Song LZ**, **Porter P**, **Putluri N**, **Salas R**, **Gilbert BE**, **Levental I**, **Campen MJ**, **Corry DB**, **Kheradmand F.** Electronic cigarettes disrupt lung lipid homeostasis and innate immunity independent of nicotine. *J Clin Invest* 129: 4290–4304, 2019. doi:10.1172/JCI128531.
9. **Polosa R**, **Cibella F**, **Caponnetto P**, **Maglia M**, **Prosperini U**, **Russo C**, **Tashkin D.** Health impact of E-cigarettes: a prospective 3.5-year study of regular daily users who have never smoked. *Sci Rep* 7: 13825, 2017. doi:10.1038/s41598-017-14043-2.
10. **Reinikovaite V**, **Rodriguez IE**, **Karoor V**, **Rau A**, **Trinh BB**, **Deleyiannis FW**, **Taraseviciene-Stewart L.** The effects of electronic cigarette vapour on the lung: direct comparison to tobacco smoke. *Eur Respir J* 51: 1701661, 2018. doi:10.1183/13993003.01661-2017.
11. **Singh KP**, **Lawyer G**, **Muthumalage T**, **Maremanda KP**, **Khan NA**, **McDonough SR**, **Ye D**, **McIntosh S**, **Rahman I.** Systemic biomarkers in electronic cigarette users: implications for noninvasive assessment of vaping-associated pulmonary injuries. *ERJ Open Res* 5: 00182-2019, 2019. doi:10.1183/23120541.00182-2019.
12. **Chaumont M**, **de Becker B**, **Zaher W**, **Culie A**, **Deprez G**, **Melot C**, **Reye F**, **Van Antwerpen P**, **Delporte C**, **Debbas N**, **Boudjeltia KZ**, **van de Borne P.** Differential effects of e-cigarette on microvascular endothelial function, arterial stiffness and oxidative stress: a randomized crossover trial. *Sci Rep* 8: 10378, 2018. doi:10.1038/s41598-018-28723-0.
13. **Fuster V**, **Moreno PR**, **Fayad ZA**, **Corti R**, **Badimon JJ.** Atherothrombosis and high-risk plaque: part I: evolving concepts. *J Am Coll Cardiol* 46: 937–954, 2005. doi:10.1016/j.jacc.2005.03.074.
14. **Kuntic M**, **Oelze M**, **Steven S**, **Kroller-Schon S**, **Stamm P**, **Kalinovic S**, **Frenis K**, **Vujacic-Mirski K**, **Jimenez B**, **Kvandova MT**, **Filippou M**, **Al Zuabi K**, **Bruckl A**, **Hahad V**, **Daub O**, **Varveri S**, **Gori F**, **Huesmann T**, **Hoffmann R**, **Schmidt T**, **Keaney Jf FP**, **Daiber A**, **Munzel T.** Short-term e-cigarette vapour exposure causes vascular oxidative stress and dysfunction: evidence for a close connection to brain damage and a key role of the phagocytic NADPH oxidase (NOX-2). *Eur Heart J* 46: 2472–2483, 2019. [https://pubmed.ncbi.nlm.nih.gov/31715629/].
15. **Song MA**, **Reisinger SA**, **Freudenheim JL**, **Brasky TM**, **Mathe EA**, **McElroy JP**, **Nickerson QA**, **Weng DY**, **Wewers MD**, **Shields PG.** Effects of electronic cigarette constituents on the human lung: a Pilot Clinical Trial. *Cancer Prev Res (Phila)* 13: 145–152, 2020. doi:10.1158/1940-6207.CAPR-19-0400.
16. **Wolkart G**, **Kollau A**, **Stessel H**, **Russwurm M**, **Koesling D**, **Schrammel A**, **Schmidt K**, **Mayer B.** Effects of flavoring compounds used in electronic cigarette refill liquids on endothelial and vascular function. *PLoS One* 14: e0222152, 2019. e0222152doi:10.1371/journal.pone.0222152.
17. **Laube BL**, **Afshar-Mohajer N**, **Koehler K**, **Chen G**, **Lazarus P**, **Collaco JM**, **McGrath-Morrow SA.** Acute and chronic in vivo effects of exposure to nicotine and propylene glycol from an E-cigarette on mucociliary clearance in a murine model. *Inhal Toxicol* 29: 197–205, 2017. doi:10.1080/08958378.2017.1336585.
18. **Reidel B**, **Radicioni G**, **Clapp PW**, **Ford AA**, **Abdelwahab S**, **Rebuli ME**, **Haridass P**, **Alexis NE**, **Jaspers I**, **Kesimer M.** E-cigarette use causes a unique innate immune response in the lung, involving increased neutrophilic activation and altered mucin secretion. *Am J Respir Crit Care Med* 197: 492–501, 2018. doi:10.1164/rccm.201708-1590OC.
19. **Chatterjee S**, **Tao JQ**, **Johncola A**, **Guo W**, **Caporale A**, **Langham MC**, **Wehrli FW.** Acute exposure to e-cigarettes causes inflammation and pulmonary endothelial oxidative stress in nonsmoking, healthy young subjects. *Am J Physiol Lung Cell Mol Physiol* 317: L155–L166, 2019. doi:10.1152/ajplung.00110.2019.
20. **Caporale A**, **Langham MC**, **Guo W**, **Johncola A**, **Chatterjee S**, **Wehrli FW.** Acute effects of electronic cigarette aerosol inhalation on vascular function detected at quantitative MRI. *Radiology* 293: 97–106, 2019. 190562doi:10.1148/radiol.2019190562.
21. **Chen W**, **Wang P**, **Ito K**, **Fowles J**, **Shusterman D**, **Jaques PA**, **Kumagai K.** Measurement of heating coil temperature for e-cigarettes with a "top-coil" clearomizer. *PLoS One* 13: e0195925, 2018. doi:10.1371/journal.pone.0195925.
22. **Vaping Daily**. Communication page. https://vapingdaily.com/nicotine-free-vapes/2020.
23. **St Helen G**, **Ross KC**, **Dempsey DA**, **Havel CM**, **Jacob P**, **Benowitz NL 3rd.** Nicotine delivery and vaping behavior during ad libitum e-cigarette access**.** *Tobacco Reg Sci* 2: 363–376, 2016. doi:10.18001/TRS.2.4.8.
24. **Farsalinos KE**, **Spyrou A**, **Stefopoulos C**, **Tsimopoulou K**, **Kourkoveli P**, **Tsiapras D**, **Kyrzopoulos S**, **Poulas K**, **Voudris V.** Nicotine absorption from electronic cigarette use: comparison between experienced consumers (vapers) and naive users (smokers). *Sci Rep* 5: 11269, 2015. doi:10.1038/srep11269.
25. **Behar RZ**, **Hua M**, **Talbot P.** Puffing topography and nicotine intake of electronic cigarette users. *PLoS One* 10: e0117222, 2015. doi:10.1371/journal.pone.0117222.
26. **Chaumont M**, **van de Borne P**, **Bernard A**, **Van Muylem A**, **Deprez G**, **Ullmo J**, **Starczewska E**, **Briki R**, **de Hemptinne Q**, **Zaher W**, **Debbas N.** Fourth generation e-cigarette vaping induces transient lung inflammation and gas exchange disturbances: results from two randomized clinical trials. *Am J Physiol Lung Cell Mol Physiol* 316: L705–L719, 2019. doi:10.1152/ajplung.00492.2018.
27. **Ghasemi A**, **Zahediasl S**, **Azizi F.** Elevated nitric oxide metabolites are associated with obesity in women. *Arch Iran Med* 16: 521–525, 2013 .
28. **Zahedi Asl S**, **Ghasemi A**, **Azizi F.** Serum nitric oxide metabolites in subjects with metabolic syndrome. *Clin Biochem* 41: 1342–1347, 2008. doi:10.1016/j.clinbiochem.2008.08.076.
29. **Giustarini D**, **Rossi R**, **Milzani A**, **Dalle-Donne I.** Nitrite and nitrate measurement by Griess reagent in human plasma: evaluation of interferences and standardization. *Methods Enzymol* 440: 361–380, 2008. doi:10.1016/S0076-6879(07)00823-3.
30. **Krump-Konvalinkova V**, **Bittinger F**, **Unger RE**, **Peters K**, **Lehr HA**, **Kirkpatrick CJ.** Generation of human pulmonary microvascular endothelial cell lines. *Lab Invest* 81: 1717–1727, 2001. doi:10.1038/labinvest.3780385.
31. **Pietrofesa RA**, **Woodruff P**, **Hwang WT**, **Patel P**, **Chatterjee S**, **Albelda SM**, **Christofidou-Solomidou M.** The synthetic lignan secoisolariciresinol diglucoside prevents asbestos-induced NLRP3 inflammasome activation in murine macrophages. *Oxid Med Cell Longev* 2017: 1–14, 2017. doi:10.1155/2017/7395238.
32. **Esterberg R**, **Linbo T**, **Pickett SB**, **Wu P**, **Ou HC**, **Rubel EW**, **Raible DW.** Mitochondrial calcium uptake underlies ROS generation during aminoglycoside-induced hair cell death. *J Clin Invest* 126: 3556–3566, 2016. doi:10.1172/JCI84939.
33. **Browning E**, **Wang H**, **Hong N**, **Yu K**, **Buerk DG**, **DeBolt K**, **Gonder D**, **Sorokina EM**, **Patel P**, **De Leon DD**, **Feinstein SI**, **Fisher AB**, **Chatterjee S.** Mechanotransduction drives post ischemic revascularization through K(ATP) channel closure and production of reactive oxygen species. *Antioxid Redox Signal* 20: 872–886, 2014. doi:10.1089/ars.2012.4971.
34. **Tao JQ**, **Sorokina EM**, **Vazquez Medina JP**, **Mishra MK**, **Yamada Y**, **Satalin J**, **Nieman GF**, **Nellen JR**, **Beduhn B**, **Cantu E**, **Habashi NM**, **Jungraithmayr W**, **Christie JD**, **Chatterjee S.** Onset of inflammation with ischemia: implications for donor lung preservation and transplant survival. *Am J Transplant* 16: 2598–2611, 2016. doi:10.1111/ajt.13794.

35. **Langham MC**, **Wehrli**, **FW.** Simultaneous mapping of temporally-resolved blood flow velocity and oxygenation in femoral artery and vein during reactive hyperemia. *J Cardiovasc Magn Reson* 13: 66, 2011. doi:10.1186/1532-429X-13-66.
36. **Langham MC**, **Li C**, **Englund EK**, **Chirico EN**, **Mohler ER 3rd**, **Floyd TF**, **Wehrli FW.** Vessel-wall imaging and quantification of flow-mediated dilation using water-selective 3D SSFP-echo. *J Cardiovasc Magn Reson* 15: 100, 2013. doi:10.1186/1532-429X-15-100.
37. **Brian JE. Jr**, Carbon dioxide and the cerebral circulation**.** *Anesthesiology* 88: 1365–1386, 1998. doi:10.1097/00000542-199805000-00029.
38. **Rodgers ZB**, **Jain V**, **Englund EK**, **Langham MC**, **Wehrli FW.** High temporal resolution MRI quantification of global cerebral metabolic rate of oxygen consumption in response to apneic challenge. *J Cereb Blood Flow Metab* 33: 1514–1522, 2013. doi:10.1038/jcbfm.2013.110.
39. **Langham MC**, **Li C**, **Wehrli FW.** Non-triggered quantification of central and peripheral pulse-wave velocity. *J Cardiovasc Magn Reson* 13: 81, 2011. doi:10.1186/1532-429X-13-81.
40. **Noel J**, **Wang H**, **Hong N**, **Tao JQ**, **Yu K**, **Sorokina EM**, **Debolt K**, **Heayn M**, **Rizzo V**, **Delisser H**, **Fisher AB**, **Chatterjee S.** PECAM-1 and caveolae form the mechanosensing complex necessary for NOX2 activation and angiogenic signaling with stopped flow in pulmonary endothelium. *Am J Physiol Lung Cell Mol Physiol* 305: L805–L818, 2013. doi:10.1152/ajplung.00123.2013.
41. **Langham MC**, **Englund EK**, **Mohler ER**, **Li C**, **Rodgers ZB**, **Floyd TF**, **Wehrli**, **FW.** Quantitative CMR markers of impaired vascular reactivity associated with age and peripheral artery disease. *J Cardiovasc Magn Reson* 15: 17, 2013. doi:10.1186/1532-429X-15-17.
42. **Biondi-Zoccai G**, **Sciarretta S**, **Bullen C**, **Nocella C**, **Violi F**, **Loffredo L**, **Pignatelli P**, **Perri L**, **Peruzzi M**, **Marullo AG**, **Falco Chimenti DE**, **Cammisotto I**, **Valenti V**, **Coluzzi V**, **Cavarretta F**, **Carrizzo E**, **Prati A**, **Carnevale F**, **Frati RD.** Acute effects of heat-not-burn, electronic vaping, and traditional tobacco combustion cigarettes: The Sapienza University of Rome-Vascular Assessment of Proatherosclerotic Effects of Smoking (SUR-VAPES) 2 Randomized Trial. *J Am Heart Assoc* 8: e010455, 2019.
43. **Carnevale R**, **Sciarretta S**, **Violi F**, **Nocella C**, **Loffredo L**, **Perri L**, **Peruzzi M**, **Marullo AG**, **De Falco E**, **Chimenti I**, **Valenti V**, **Biondi-Zoccai G**, **Frati G.** Acute impact of tobacco vs electronic cigarette smoking on oxidative stress and vascular function. *Chest* 150: 606–612, 2016. doi:10.1016/j.chest.2016.04.012.
44. **Higashi Y**, **Maruhashi T**, **Noma K**, **Kihara Y.** Oxidative stress and endothelial dysfunction: clinical evidence and therapeutic implications. *Trends Cardiovasc Med* 24: 165–169, 2014. doi:10.1016/j.tcm.2013.12.001.
45. **Simionescu M.** Implications of early structural-functional changes in the endothelium for vascular disease. *Arterioscler Thromb Vasc Biol* 27: 266–274, 2007. doi:10.1161/01.ATV.0000253884.13901.e4.
46. **Fetterman JL**, **Keith RJ**, **Palmisano JN**, **McGlasson KL**, **Weisbrod RM**, **Majid S**, **Bastin R**, **Stathos MM**, **Stokes AC**, **Robertson RM**, **Bhatnagar A**, **Hamburg NM.** Alterations in vascular function associated with the use of combustible and electronic cigarettes. *J Am Heart Assoc* 9: e014570, 2020. doi:10.1161/JAHA.119.014570.
47. **Olfert IM**, **DeVallance E**, **Hoskinson H**, **Branyan KW**, **Clayton S**, **Pitzer CR**, **Sullivan DP**, **Breit MJ**, **Wu Z**, **Klinkhachorn P**, **Mandler WK**, **Erdreich BH**, **Ducatman BS**, **Bryner RW**, **Dasgupta P**, **Chantler PD.** Chronic exposure to electronic cigarettes results in impaired cardiovascular function in mice. *J Appl Physiol (1985)* 124: 573–582, 2018. doi:10.1152/japplphysiol.00713.2017.
48. **Vlachopoulos C**, **Ioakeimidis N**, **Abdelrasoul M**, **Terentes-Printzios D**, **Georgakopoulos C**, **Pietri P**, **Stefanadis C**, **Tousoulis D.** Electronic cigarette smoking increases aortic stiffness and blood pressure in young smokers. *J Am Coll Cardiol* 67: 2802–2803, 2016. doi:10.1016/j.jacc.2016.03.569.
49. **Gabay C**, **Kushner I.** Acute-phase proteins and other systemic responses to inflammation. *N Engl J Med* 340: 448–454, 1999. doi:10.1056/NEJM199902113400607.
50. **Scaffidi P**, **Misteli T**, **Bianchi ME.** Release of chromatin protein HMGB1 by necrotic cells triggers inflammation. *Nature* 418: 191–195, 2002. doi:10.1038/nature00858.
51. **Gibot S**, **Massin F**, **Cravoisy A**, **Barraud D**, **Nace L**, **Levy B**, **Bollaert PE.** High-mobility group box 1 protein plasma concentrations during septic shock. *Intensive Care Med* 33: 1347–1353, 2007. doi:10.1007/s00134-007-0691-2.
52. **Zheng W**, **Shi H**, **Chen Y**, **Xu Z**, **Chen J**, **Jin L.** Alteration of serum high-mobility group protein 1 (HMGB1) levels in children with enterovirus 71-induced hand, foot, and mouth disease. *Medicine (Baltimore)* 96: e6764, 2017. doi:10.1097/MD.0000000000006764.
53. **Chen H**, **Zhang X**, **Liao N**, **Mi L**, **Peng Y**, **Liu B**, **Zhang S**, **Wen F.** Enhanced expression of nlrp3 inflammasome-related inflammation in diabetic retinopathy. *Invest Ophthalmol Vis Sci* 59: 978–985, 2018. doi:10.1167/iovs.17-22816.
54. **Kerr N**, **Garcia-Contreras M**, **Abbassi S**, **Mejias NH**, **Desousa BR**, **Ricordi C**, **Dietrich WD**, **Keane RW**, **de Rivero Vaccari JP.** Inflammasome proteins in serum and serum-derived extracellular vesicles as biomarkers of stroke. *Front Mol Neurosci* 11: 309, 2018. doi:10.3389/fnmol.2018.00309.
55. **Turhan H**, **Saydam GS**, **Erbay AR**, **Ayaz S**, **Yasar AS**, **Aksoy Y**, **Basar N**, **Yetkin E.** Increased plasma soluble adhesion molecules; ICAM-1, VCAM-1, and E-selectin levels in patients with slow coronary flow. *Int J Cardiol* 108: 224–230, 2006. doi:10.1016/j.ijcard.2005.05.008.
56. **Aldaham S**, **Foote JA**, **Chow HH**, **Hakim IA.** Smoking status effect on inflammatory markers in a randomized trial of current and former heavy smokers. *Int J Inflam* 2015: 1–6, 2015. doi:10.1155/2015/439396.
57. **Tracy RP**, **Psaty BM**, **Macy E**, **Bovill EG**, **Cushman M**, **Cornell ES**, **Kuller LH.** Lifetime smoking exposure affects the association of C-reactive protein with cardiovascular disease risk factors and subclinical disease in healthy elderly subjects. *Arterioscler Thromb Vasc Biol* 17: 2167–2176, 1997. doi:10.1161/01.ATV.17.10.2167.
58. **Hage FG**, **Szalai AJ.** C-reactive protein gene polymorphisms, C-reactive protein blood levels, and cardiovascular disease risk. *J Am Coll Cardiol* 50: 1115–1122, 2007. doi:10.1016/j.jacc.2007.06.012.
59. **Devaraj S**, **Venugopal S**, **Jialal I.** Native pentameric C-reactive protein displays more potent pro-atherogenic activities in human aortic endothelial cells than modified C-reactive protein. *Atherosclerosis* 184: 48–52, 2006. doi:10.1016/j.atherosclerosis.2005.03.031.
60. **Eisenhardt SU**, **Thiele JR**, **Bannasch H**, **Stark GB**, **Peter K.** C-reactive protein: how conformational changes influence inflammatory properties. *Cell Cycle* 8: 3885–3892, 2009. doi:10.4161/cc.8.23.10068.
61. **Papas AM.** Determinants of antioxidant status in humans. *Lipids* 31, Suppl: S77–82, 1996. doi:10.1007/BF02637055.
62. **Kornacki J**, **Koz˙lik J**, **Dubiel M**, **Skrzypczak , J.** [Estimation of oxidative stress and its correlation with uterine arteries Doppler velocimetry in women with preeclampsia] *Ginekol Pol* 75: 681–691, 2004.
63. **Kooijman M**, **Thijssen DH**, **de Groot PC**, **Bleeker MW**, **van Kuppevelt HJ**, **Green DJ**, **Rongen GA**, **Smits P**, **Hopman , MT.** Flow-mediated dilatation in the superficial femoral artery is nitric oxide mediated in humans. *J Physiol* 586: 1137–1145, 2008. doi:10.1113/jphysiol.2007.145722.
64. **Beckman JS**, **Koppenol**, **WH.** Nitric oxide, superoxide, and peroxynitrite: the good, the bad, and ugly. *Am J Physiol Cell Physiol* 271: C1424–C1437, 1996. doi:10.1152/ajpcell.1996.271.5.C1424.
65. **Joshi MS**, **Ferguson TB Jr**, **Han TH**, **Hyduke DR**, **Liao JC**, **Rassaf T**, **Bryan N**, **Feelisch M**, **Lancaster JR.** Nitric oxide is consumed, rather than conserved, by reaction with oxyhemoglobin under physiological conditions. *Proc Natl Acad Sci U S A* 99: 10341–10346, 2002. doi:10.1073/pnas.152149699.
66. **Kovacs I**, **Toth J**, **Tarjan J**, **Koller A.** Correlation of flow mediated dilation with inflammatory markers in patients with impaired cardiac function. Beneficial effects of inhibition of ACE. *Eur J Heart Fail* 8: 451–459, 2006. doi:10.1016/j.ejheart.2005.10.011.
67. **Gao D**, **Shao J**, **Jin W**, **Xia X**, **Qu Y.** Correlations of serum cystatin C and hs-CRP with vascular endothelial cell injury in patients with systemic lupus erythematosus. *Panminerva Med* 60: 151–155, 2018. doi:10.23736/S0031-0808.18.03466-3.
68. **Bleakley C**, **Hamilton PK**, **Pumb R**, **Harbinson M**, **McVeigh GE.** Endothelial function in hypertension: victim or culprit? *J Clin Hypertens* 17: 651–654, 2015. doi:10.1111/jch.12546.
69. **Wu PH**, **Rodriguez-Soto AE**, **Rodgers ZB**, **Englund EK**, **Wiemken A**, **Langham MC**, **Detre JA**, **Schwab RJ**, **Guo W**, **Wehrli FW.** MRI evaluation of cerebrovascular reactivity in obstructive sleep apnea. *J*

Cereb Blood Flow Metab 40: 1328–1337, 2020. doi:10.1177/0271678X19862182.

70. **Schweitzer KS**, **Chen SX**, **Law S**, **Van Demark M**, **Poirier C**, **Justice MJ**, **Hubbard WC**, **Kim ES**, **Lai X**, **Wang M**, **Kranz WD**, **Carroll CJ**, **Ray BD**, **Bittman R**, **Goodpaster J**, **Petrache I.** Endothelial disruptive proinflammatory effects of nicotine and e-cigarette vapor exposures. *Am J Physiol Lung Cell Mol Physiol* 309: L175–L187, 2015. doi:10.1152/ajplung.00411.2014.
71. **Voos N**, **Smith D**, **Kaiser L**, **Mahoney MC**, **Bradizza CM**, **Kozlowski LT**, **Benowitz NL**, **O'Connor RJ**, **MI G.** Effect of e-cigarette flavors on nicotine delivery and puffing topography: results from a randomized clinical trial of daily smokers. *Psychopharmacology (Berl)* 237: 491–502, 2020. doi:10.1007/s00213-019-05386-x.
72. **Chapman DG**, **Casey DT**, **Ather JL**, **Aliyeva M**, **Daphtary N**, **Lahue KG**, **van der Velden JL**, **Janssen-Heininger YM**, **Irvin CG.** The effect of flavored e-cigarettes on murine allergic airways disease. *Sci Rep* 9: 13671, 2019. doi:10.1038/s41598-019-50223-y.
73. **Szafran BN**, **Pinkston R**, **Perveen Z**, **Ross MK**, **Morgan T**, **Paulsen DB**, **Penn AL**, **Kaplan BLF**, **Noel A.** Electronic-cigarette vehicles and flavoring affect lung function and immune responses in a murine model. *Int J Mol Sci* 21: 13671, 2020. [https://pubmed.ncbi.nlm.nih.gov/32825651/].

Figure S1

Changes in Biomarkers (ΔY) and MRI metrics (ΔZ); (Δ=post-pre)

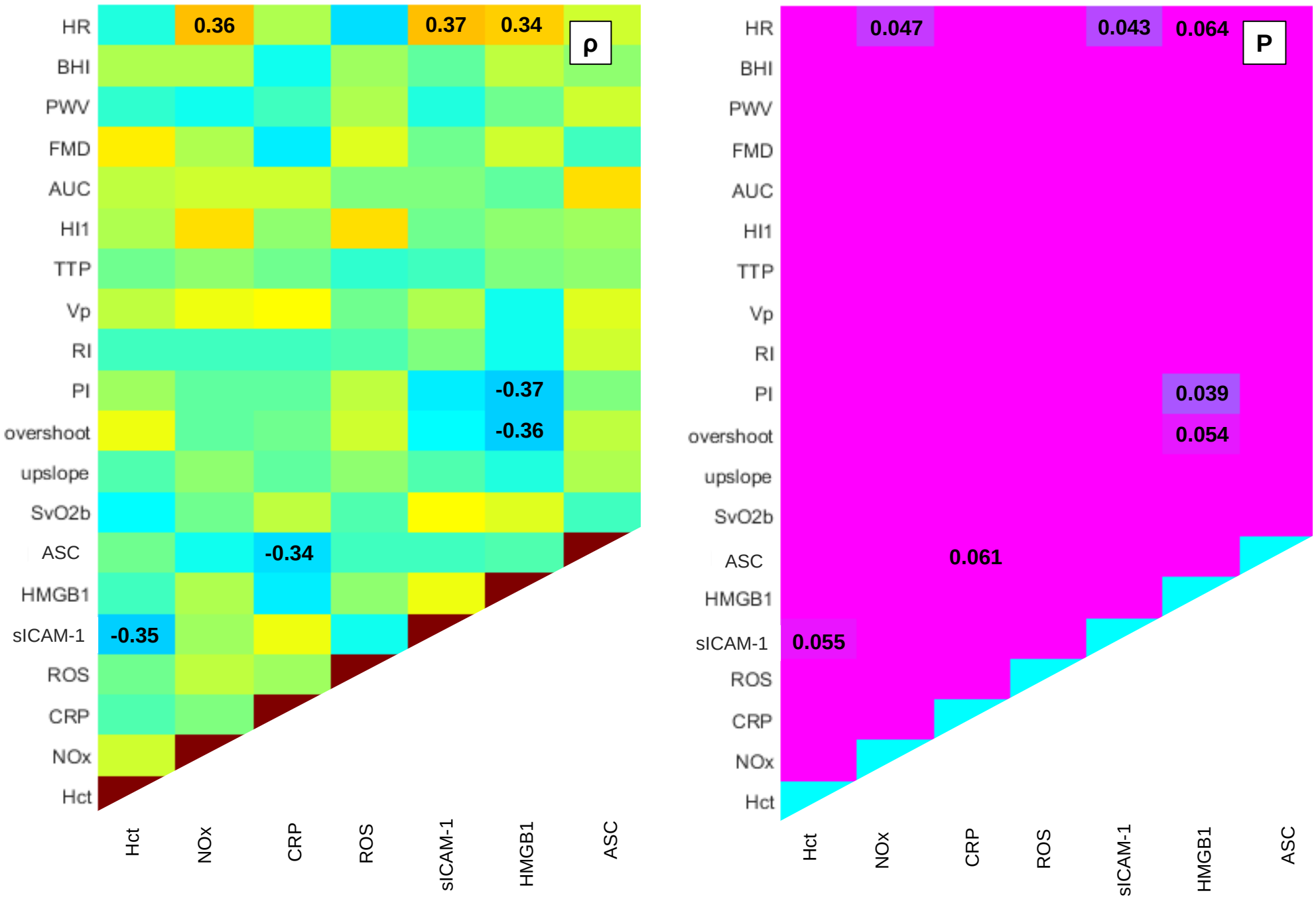

Figure S2

Changes in Biomarkers (ΔY, Y=ln(y)) and MRI metrics (ΔZ); (Δ=post-pre)

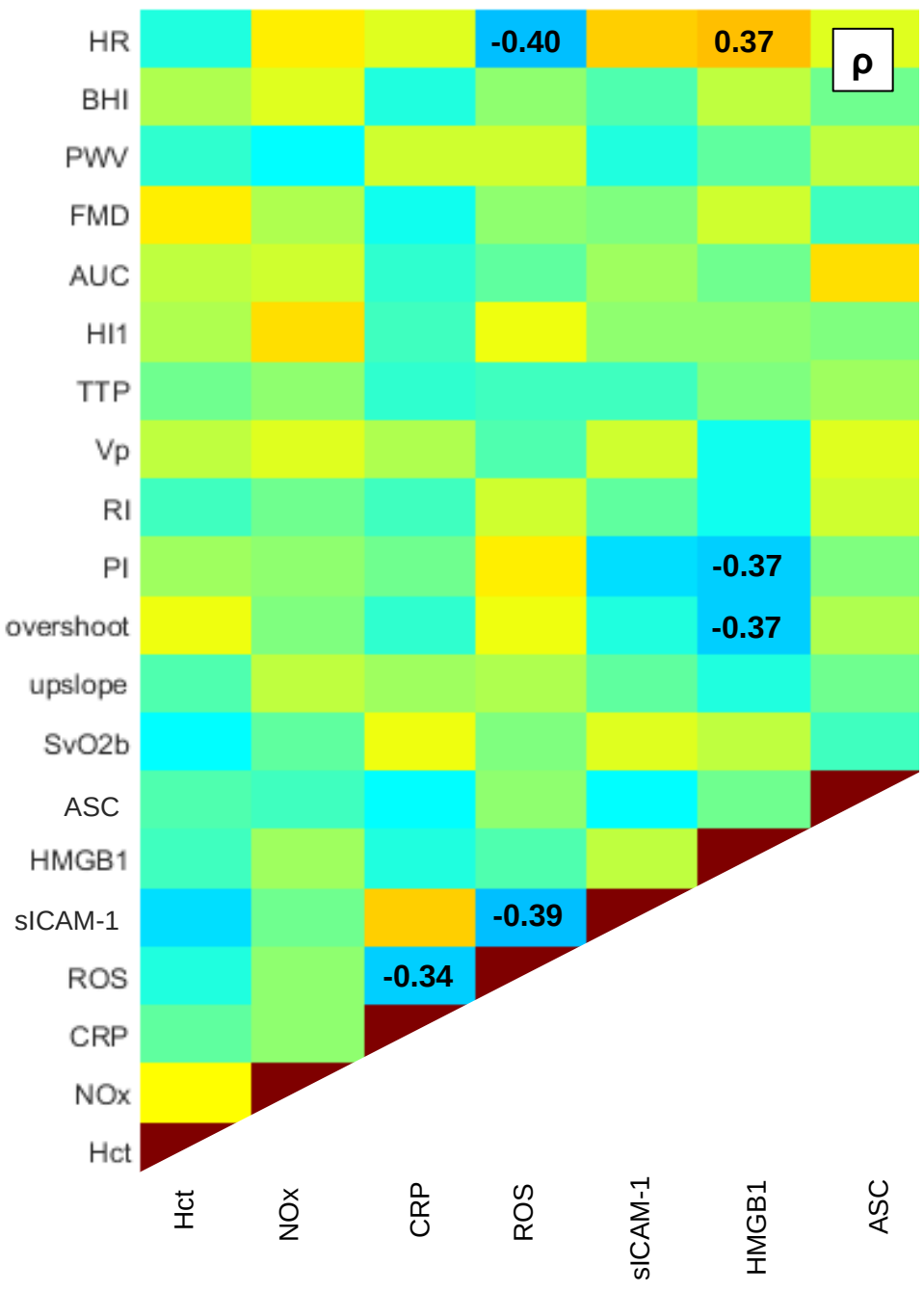

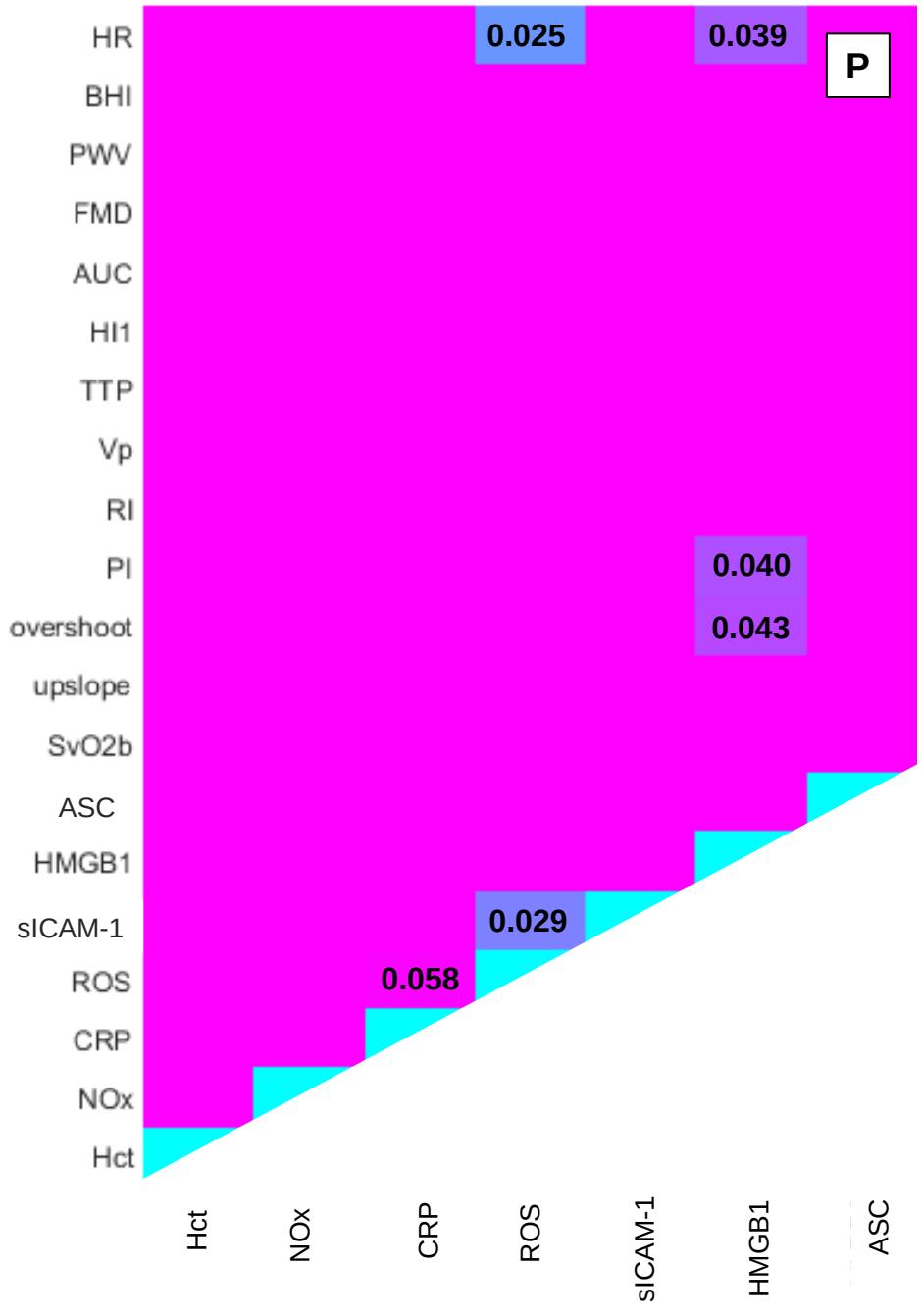

Supplementary Table 1. – Stepwise regression analysis coefficients not shown in the main manuscript

	Regression model	**Coefficients (non standardized) ± std Dev**	**95% CI**	**Significance (P)**
overshoot	Overshoot = a*HMBG1 + k	a = -14.48 ± 5.02 k = 65.84 ± 13.06	(-24.79, -4.17) (39.05, 92.63)	0.008 <0.0001
HI	HI = a*HMBG1 + k	a = 6.02 ± 2.89 k = -4.45 ± 7.50	(0.1, 11.94) (-19.84, 10.95)	0.047 0.56
Δovershoot	Δovershoot = a* ΔROS + k	a = 9.57 ± 3.73 k = 3.08 ± 3.10	(1.92, 17.22) (-3.29, 9.44)	0.016 0.33
ΔPI	ΔPI = a* ΔROS + k	a = 3.46 ± 1.31 k = 0.081 ± 1.09	(0.77, 6.15) (-2.16, 2.32)	0.013 0.94
ΔBHI	ΔBHI = a*BMI + k	a = 0.008 ± 0.004 k = -2.06 ± 0.087	(0, 0.016) (-0.39, -0.027)	0.039 0.025

BHI = breathold index; BMI = body mass index; HI = hyperemic index; PI = pulsatility index